ABSTRACT

Title of Document: PROBING POSTURAL STABILITY MECHANISMS IN LOCOMOTION

David M. Logan, M.A., 2009

Directed By: Professor John Jeka, Department of Kinesiology

It is not currently known if those upright stability mechanisms utilized in standing posture are present in locomotion. In this investigation, subjects walked or stood on a treadmill in three speed conditions (posture, 1 km/h, 5 km/h) in front of a visual scene consisting of randomly oriented triangles. The triangles translated in the anterior-posterior (A/P) direction in either a low or high amplitude condition. Frequency response functions (FRFs) of both the A/P displacement of bilateral kinematic markers and their corresponding segment angles in response to the visual scene translations were computed. Gain and phase of these FRFs had consistent responses in high amplitude visual conditions in the trunk (hip and shoulder displacements, trunk angle), which motivated further comparisons within the trunk during posture and locomotion. In doing so, the postural processes of orientation and equilibrium control were teased apart during locomotion.

PROBING POSTURAL STABILITY MECHANISMS IN LOCOMOTION

By

David M. Logan

Thesis submitted to the Faculty of the Graduate School of the
University of Maryland, College Park, in partial fulfillment
of the requirements for the degree of
Master of Arts
2009

Advisory Committee:
Professor John Jeka, Ph.D., Chair
Professor Jane E. Clark, Ph.D.
Assistant Professor Timothy Kiemel, Ph.D.

Acknowledgements

I would like to thank all of those who have helped create this document in some way or another, especially:

- My family, particularly my parents Mike and Teresa, for all the support and guidance they have provided over the years.
- Beth, for being at my side wherever science may take us.
- John Jeka, for his support, advice, and perspective.
- Tim Kiemel and Jane E. Clark for serving on my committee and providing valuable feedback and guidance.
- Francesco Lacquaniti and Yuri Ivanenko for their support and guidance.
- Nadia Dominici and Germana Cappellini for their assistance and patience during data collection.
- Peter Agada, for his assistance in technical matters.
- Eric Anson, for the many discussions about this complicated behavior.
- Leslie Allison, Rob Creath and Mark Saffer for mentorship along the way.

Table of Contents

Acknowledgements ii
List of Tables v
List of Figures vi
Chapter 1: Introduction 1
Specific Aims 4
Thesis Organization 5
Chapter 2: Review of Literature 7
Biomechanics and Standard Measures of Locomotion 7
Dynamic Stability 11
Visual modulation of Locomotion 13
Sensory Re-weighting in Posture 18
Sensory Re-weighting in Locomotion 19
Posture and Locomotion: Common use of Visual Information? 21
Freezing Illusion 23
Chapter 3: Pilot Investigation 27
Methods 27
Apparatus 27
Procedures 28
Analysis 29
Preliminary Findings 30
Power Spectral Density and Locomotive Frequency 31
Complex Coherence 34
Gain and Phase 35
Chapter 4: Intra-modal Reweighting 38
Methods 38
Subjects 38
Apparatus 38
Procedures 41
Analysis 41
Statistics 43
Results 44
Gain and Phase: Displacements 44
Gain and Phase: Segment Angles 48
FRFs at the stride frequency 50
Chapter 5: "Visual Influence on Trunk Stability during Locomotion" 52
Methods 56
Subjects 56
Apparatus 56
Procedures 58
Analysis 59

Statistics 61
Results 62
Phase dependence: Trunk-Leg Segments 62
Gain-phase 65
Kinematic variance and scene stabilization 70
Discussion 73
Gain & Phase: Posture vs. Locomotion 73
Effect of Visual Amplitude 75
Effects of Speed 77
Motion variance, scene stabilization and reweighting 78
Chapter 6: Leg-Trunk Coordination 82
Methods 82
Analysis 82
Statistics 83
Results 83
Chapter 7: General Discussion 87
Intra-modal reweighting not evident in locomotion 87
Trunk-leg coordination 89
Conclusion and Future Directions 91
Appendix 1: Consent Form 93
Bibliography 97

List of Tables

Table 3.1. Successful Trials in Pilot Study……..…….28

Table 5.1. General Gait Measures…….……...72

List of Figures

Figure 3.1. Time Series of AP Displacement……..30

Figure 3.2. PSDs of Head……31

Figure 3.3. Locomotion Frequency……..32

Figure 3.4. PSDs of Head with Locomotion Frequency……..33

Figure 3.5. Mean FRF: Posture……...36

Figure 3.6. Mean FRF: Five km/h……..37

Figure 4.1. Experimental Setup……...39

Figure 4.2. Stimuli……...40

Figure 4.3. Gain and Phase of Ankle: Amplitude Effects……44

Figure 4.4. Gain and Phase of Knee: Amplitude Effects…….45

Figure 4.5. Gain and Phase of Hip: Amplitude Effects……...46

Figure 4.6. Gain and Phase of Shoulder: Amplitude Effects……...46

Figure 4.7. Gain and Phase of Leg Angle: Amplitude Effects……48

Figure 4.8. Gain and Phase of Trunk Angle: Amplitude Effects…….49

Figure 4.9. FRF at Gait Frequency……..50

Figure 5.1. Cross-covariance……...63

Figure 5.2. Phase Dependent Cross-covariance……...65

Figure 5.3 Gain and Phase: Amplitude Effects……66

Figure 5.4 Gain and Phase: Translation versus Orientation……67

Figure 5.5. Interaction of Speed and Trunk Kinematics……..69

Figure 5.6. Variance: Position and Velocity Variance……71

Figure 6.1. Complex Coherence of Leg and Trunk…….84

Figure 6.2. Normalized Complex Coherence of Leg and Trunk…….85

Chapter 1: Introduction

As the body's segments perpetuate movement during locomotion, there is noticeable oscillation in all planes that poses a problem to maintaining balance. As the body's center of gravity fluctuates in and out of its support base, there must be processes in place to counter the destabilizing effects of a massive trunk and swinging legs (Mackinnon & Winter, 1993). In standing posture, there are properties of sensory fusion in place to "re-weight" the amount of feedback from one stream of information about the environment to another in an effort to thwart erroneous sensory information. One would suppose the properties of sensory response are more complicated in locomotion, but evidence suggests that postural and locomotive responses to share common features (Kay & Warren, Jr., 2001).

From a neurophysiology standpoint, the anatomical pieces are in place for locomotive behavior to receive modulatory visual input (Rossignol et al., 2006). Indeed, manipulations of visual information have been shown to have an effect on heading, steering, head stability, head-trunk interactions and body sway coupling during locomotion (Vallis & Patla, 2004; Hollands et al., 2002; Schubert et al., 2003; Prokop et al., 1997; Warren et al., 1996). These studies reveal a clear need for an investigation of the degree of which visual information is used to actually stabilize the body's segments upright during locomotion.

Undoubtedly, sensory information is vital to the central nervous system's ability to stabilize the human body during bipedal stance. With regular updating of visual, somatosensory, and vestibular information the body is able to stabilize itself vertical to earth. Several studies have shown that intact subjects actively seek out

alternative sources of sensory information in destabilizing environments while patients compensate for sensory deficits to stabilize posture (Nashner, 1982). Few studies that specifically probe postural sway in the frequency domain indicate that the process of re-weighting (inter-modality) is termed so because of strong coupling of one sensory drive with postural sway (up-weighting) in conjunction with weak coupling of another sensory modality with postural sway (down-weighting). Additionally, intra-modal reweighting occurs in posture when increasing the stimulus amplitude of the same sensory modality causes a greater increase in coupling to that stimulus (Oie, Kiemel, & Jeka, 2002; Peterka, 2002).

A detailed account of intra-modal reweighting has not been reported in locomotion, and experiments that investigate inter-sensory interactions suggest it is possible. Deshpande and Patla have found an up-weighting of the vestibular system at the initial phase of a walking followed by a dominance of vision when approaching a target (Deshpande & Patla, 2005). They've also found that younger adults compared to older adults are able to up-weight to vision due to intact sensory re-weighting mechanisms (Deshpande & Patla, 2007). Varraine and colleagues have found that spectral amplitude of walking speed at the frequency of visual stimulation was much higher in a condition with both visual and force perturbations compared to visual perturbations alone (Varraine, Bonnard & Pailhous, 2006). More directly related to intra-modal reweighting, mean sway amplitude does not increase proportionally with translational amplitude of a visual scene during locomotion (Warren et al., 1996). This finding coupled with the results of inter-modal investigations suggests that an intra-modal reweighting process occurs in locomotion.

Before paradigms are adjusted and experiments that delve into this comparison are conducted, there are complexities of locomotion that must be considered. When attempting to understand the sensory fusion process, the speed at which the body moves must be taken into account. During slower speeds, there is growing evidence that the body is more dynamically stable and that different segments of the body have different degrees of this dynamic stability (Kang & Dingwell, 2006; England & Granata, 2006). Even though the body receives visual input in all speeds of locomotion, the degree of which this visual information is actually used to stabilize the body when speeds change is not entirely clear. In light of these studies, the sensory re-weighting of posture should be found in locomotion and should be modulated by the speed of movement.

In the process of maintaining posture upright, the ankle and hip strategies have long been thought vital to maintain postural orientation and equilibrium during perturbed stance (Horak & Macpherson, 1996). Smaller, more subtle (E.g. low frequency) perturbations tend to produce the ankle strategy while the hip strategy is elicited by those larger, more drastic changes in sensory environments. Instead of exclusive entities selected for balancing the body, there is evidence that the two strategies are always present in frequencies of sway as "co-existing excitable modes" in quiet stance (Creath, Kiemel, Horak, Peterka, & Jeka, 2005). In-phase behavior of leg and trunk angles at lower frequencies combined with anti-phase behavior at higher frequencies show that the relationship between the angles changes based on frequency of movement.

Upon the addition of sensory perturbations to these strategies, the low-frequency coherence relationship of leg and trunk segments are modulated by these sensory perturbations while the high-frequency relationship is not affected (Zhang, Kiemel, & Jeka, 2007). Thus, the higher frequency relationship is a product of the mechanical features of the two pendulum body while the low frequency relationship is subject to coordination via sensory feedback. These specific properties of the leg-trunk coordination found in posture have not been investigated in such tasks as walking or running.

Specific Aims

This research has two specific aims:

1. To investigate intra-modality reweighting in locomotion at a broad range of frequencies from .01 to 5 Hz. A low and high amplitude filtered white noise signal will be used to translate a visual scene while subjects walk on a treadmill.

Hypothesis 1: There will be a decrease in coupling to the visual drive as its amplitude increases, signified by a decrease in gain.

Hypothesis 2: There will be an interaction between intra-modal reweighting and gait speed. The well established relationship between visual amplitude and gain (higher amplitude = lower gain) will be observed during standing posture. However, at low gait speed, gain will decrease less as a function of visual amplitude when compared to standing posture. Gain will show very little change as a function of visual amplitude at the highest gait speed.

2. To investigate this intra-modal reweighting at the level of leg and trunk segment interaction.

Hypothesis 3: These re-weighting relationships will be observed in all joints from lower frequencies until the cyclical frequency of locomotion is reached. At this frequency, phase for the trunk will differ markedly from the leg segment. At higher frequencies, trunk gain will continue to decrease (indicating down-weighting of the visual input) while leg gain will no longer decrease, indicating no reweighting as its main function will be to generate locomotion.

Hypothesis 4: Simultaneous in-phase and anti-phase relationships between the trunk and leg segments will be observed during locomotion, similar to that observed during standing posture.

Thesis Organization

In the next chapter, a review of literature will discuss the use of visual information during locomotion. The biomechanics of locomotion will be introduced and will be followed by a discussion of how visual information may alter the properties of locomotion. Finally, the concept of re-weighting as applicable to posture will be discussed as well as support for re-weighting during locomotion. Chapter 3 will consist of the methods and preliminary results found during a pilot investigation. Chapter 4 will consist of the methods and results in addressing hypotheses 1-3. Chapter 5 is a self-contained manuscript investigating the difference between responses of trunk displacements and segment angle. Chapter 6 will describe the

methods and results used to investigate hypothesis 4. In the final chapter, a general discussion will describe progress made towards understanding postural stability within locomotion.

Chapter 2: Review of Literature

From the flight centers of the fly to processing centers in bipedal man, visual information is vital to the act of locomotion. Of course, the use of vision allows us to adjust our speed and direction as we move through changing environments (Dickinson et al., 2000). In this process of moving from place to place, the continuous update of visual information is also used to stabilize the body. By combining this visual information with the modalities of the vestibular and somatosensory systems throughout movement, the body is able to form a coherent perception to be utilized for neural control. Although locomotion is more biomechanically complex, with additional fluctuations in vestibular and somatosensory input, it is not clear if mechanisms used to fuse sensory input are much different than those used in standing posture. One such mechanism, sensory re-weighting, seems plausible in locomotion as it has been tested in sensory manipulations and patient populations during standing posture. This review of literature intends to review the relevant literature that leads to the investigation of sensory re-weighting in locomotion.

Biomechanics and Standard Measures of Locomotion

To discuss locomotion, one must begin with those classic measures that have afforded movement scientists a dialogue. Being an integral part of these classic measures, the gait cycle consists of stance phase and swing phase. Stance phase consists of the period when the body is in motion from heel strike until the toe lifts from the ground while swing phase is the period in which that leg is off the ground.

This stance phase can be further divided based on the direction of ground reaction forces and distinguished as early stance during flat foot and late stance at the instance of heel rise. The common definition of the gait cycle consisting of stance and swing phase refers to one limb while the gait cycle, with reference to the entire body, consists of two double support phases and two single support phases. During the double support phase, both feet are in contact with the ground and weight is shifted laterally to stabilize the body. After this lateral shift, the body is in single support as the weight-bearing foot is in contact with the ground while the other limb swings. As a general rule, the time spent in the stance phase is half the time of the gait cycle plus the time of double of support while the time in swing phase consists of half of the cycle time minus the time spent in double support (Inman, Alston, & Todd, 1981).

As the body moves through theses phases of the gait cycle, there is an almost sinusoidal pattern of vertical and lateral oscillations that occurs via characteristic movements of anatomical points. Pelvic rotation, pelvic list, and knee flexion contribute to this rhythmic locomotive pattern in early stance phase. As stance begins, the pelvis rotates from around the vertical axis from left to right approximately four degrees in each direction. In doing so, the pelvis flattens those vertical arcs of oscillation so the center of mass (com) is lowered to a less degree. Additionally, the summit of this com arc is flattened by a pelvic list (positive Trendelenberg) of the non weight-bearing leg as it contributes to the hip's abductor mechanism. Simultaneous knee flexion in the supporting limb of approximately fifteen degrees occurs as the body is passed over the feet. The knee once again fully extends right before weight-bearing during stance. In regards to the arc mentioned

previously, the knees purpose is to smooth the abrupt vertical changes that take place. Due to the rotation around the ankle joint because of the foot, knee elevation is kept at very similar heights causing the vertical motion of the hip to be smooth (Inman et al., 1981).

In regards to lateral movement, several rotations around anatomical points aid in the rhythmic motion of the body from side to side. In all, these rotations cause the body to be displaced about 4-5 cm at each stride's completion. In the transverse plane at moderate speeds, the rotating thorax and shoulders are out of phase with transverse pelvic rotations by 180° to aid in this lateral rhythm. In-phase with these pelvic rotations, the thigh and shank rotate inward at the start of the swing phase. However, the middle of stance phase marks the point when the leg begins to rotate externally until swing phase of the next stride cycle begins. As the leg rotates with the pelvis, the magnitude of rotation gets increasingly larger moving down the body from pelvis to the shank. Although the foot and ankle are able to rotate inwards unabated during the swing phase, they must succumb to the externally rotating shank during the stance phase. Thus, the ankle forms an oblique axis with the foot in the swing phase while stance phase yields such an axis with the shank. These axes coupled with dorsi-flexion at the ankle allow the ankle joint to absorb some of the oblique rotations of the shank throughout the stance phase. Additionally, the foot does not slip out of place due to the hinge action of the subtalar joint that turns internal or external rotation of the shank into pronation or supination of the foot, respectively. In sum, rotations at the joints allow for the medial-lateral oscillatory behaviors during locomotion (Inman et al., 1981).

Of course, the bulk of these observations have been focused on classifying gait in the rhythmic phase rather than the development phase or decay phase of gait. Rather, those locomotive patterns in the "steady state" rather than the process of stance speeding to gait or gait slowing to stance. With these events of locomotion clearly defined in the rhythmic phase, one is able to measure classic features of the gait cycle in terms of distance and time. In level walking, Inman and colleagues have crowned the stride as the "fundamental unit of rhythmic phase" and define it as the "sequence of motions that occurs between two consecutive repetitions of a body configuration," (Inman et al., 1981). Stride and cycle are used synonymously to determine stride frequency, which is the inverse of the time it takes to complete a full cycle. With measures of time and distance, one is able to calculate the walking speed as the stride distance divided by the stride duration or the product of the distance traveled and the stride frequency. In the normal range of walking speeds, there is a linear relationship found between stride length and frequency. As it turns out, this consistent relationship is maintained at the expense of energy. Yet, values slower or faster than found in the normal range of gait speed are considered to cause a nonlinear relationship between stride distance and frequency. In addition to stride dimensions, step dimensions reveal gait is symmetrical and such dimensions are considered in terms of a limb moving forward. The right step length, for example, is defined as the distance between heel strike of the left foot and heel strike of the right foot. These step and stride dimensions are certainly examples of classic measures used to understand the biomechanics of locomotion (Inman et al., 1981).

In processing these measures for the application of experimental paradigms, one must take into account those averages that have survived testing throughout the years. Normally, speed of locomotion is considered in terms of step frequency because this measure can offset the effect that different body types have on gait. For men, the mean speed of gait in over-ground walking is 112 steps/min found in the range of 75-140 steps/min. When referring to medium speed, men are found in the range of 100-120 steps/min. For women, the mean speed is 118 steps/min found in the normal range of 80-150 steps/min. Medium speed for women, on the other hand, is found in the range of about 115-125 steps/min (Inman et al., 1981). Additionally, one must appreciate attempts to quantify gait through frequency domain analysis. In attempting to determine the frequency content of gait, Antonsson and Mann computed the power spectra of heel strikes on a force platform. They set a rigorous standard for data collection in finding that 99% of the frequency content of gait is in the region up to 15 Hz (Antonsson & Mann, 1985). In sum, knowing the events and classic measures of gait is a precursor to understanding why keeping the body stable is such a complex task as it moves from point to point.

Dynamic Stability

In this biomechanics view of locomotion, there has been a longstanding opinion that the variability in kinematics associated with slower and faster than normal gait speeds is representative of instability (Winter, 1989). Those who apply nonlinear dynamics approaches to locomotion, on the other hand, believe in making a solid distinction between variability and stability during locomotion. Most notably Dingwell, the proponents of these approaches emphasize the continuous nature of

locomotion and describe patients who slow their gait speed in order to stabilize their bodies (Dingwell & Cusumano, 2000).

Within the discussion of locomotion stability, both local dynamic stability and global stability are relevant. Local dynamic stability in this context pertains to the ability of the body to continually stabilize itself during the infinite, small perturbations that are a natural product of walking. Global stability, in contrast, takes into account the ability of the body to stabilize itself during large perturbations like tripping (Dingwell & Marin, 2006). The general methodology in studies that estimate local dynamic stability consists of collecting several trials of kinematic data, reconstructing state spaces, and calculating average maximum finite-time Lyapunov exponents. Maximum Lyapunov exponents that are negative reveal local stability while positive maximum Lyapunov exponents diverge rapidly and support the opposite.

In one of the first studies using this analysis in locomotion, Dingwell and Cusumano found that peripheral neuropathy (NP) patients who had slower walking speeds had more locally stable gait patterns than healthy controls even though their gait was more variable (Dingwell et al., 2000). In a follow up study, gait speeds were varied below and above preferred walking speeds in young, healthy subjects to confirm the effect of gait speed on stability. They found that these maximum Lyapunov exponents were much lower at the lower speeds to further support their hypothesis. Additionally, they found that kinematic variability exhibits a quadratic behavior. In the end, they suggest that there may be a trade-off between kinematic variability and local stability (Dingwell et al., 2006).

Recent papers by Granata and England add to this genre of research by investigating the view that the trunk and swing limb are the major destabilizers of the body (MacKinnon & Winter, 1993). Again, the methods used were similar and more stabile walking dynamics equated to smaller maximum Lyapunov exponents. In this study, walking speeds were adjusted for leg length and pendulum dynamics by calculating subject-specific Froude velocities. The conditions consisted of percentages of these Froude velocities and once more, slower speeds of walking were consistent with smaller maximum Lyapunov exponents. This study also compared Lyapunov exponents at the kinematic locations and showed that the ankle was significantly more stable than the hip and the hip was significantly more stable than the knee (England & Granata, 2007). Next, the same group studied the local dynamic stability of the trunk during flexion and extension tasks in stance and found that stability declines as the rate of flexion-extension increases. In addition to the contributions of Dingwell, this set of papers reveals that local dynamic stability of a single kinematic point cannot be equated for the entire body (Granata & England, 2006). Rather, varying kinematic points are more or less stable than others throughout the act of locomotion.

Visual modulation of Locomotion

A wealth of studies has shown the effects of modulating visual input on heading and steering, head stabilization, gait velocity and body sway. In general, moving in the correct direction (steering) and direction one faces (heading) are reliant on visual information. Recent evidence suggests that steering behaviors are actually specific to the type of optic flow. In terms of type of optic flow, steering behaviors

were significantly different for type of optic flow (translation, rotation, combined) and focus of expansion (0°, ±20°, ±40°) finding that rotations of the body were not seen unless there was rotation of the visual scene. Additionally, medial-lateral shifts observed in the opposite direction of the focus of expansion (FOE) suggest that FOE may steer one's M/L components during locomotion (Sarre, Berard, Fung, & Lamontagne, 2008).

Previously, steering synergies identified in eyes open and closed conditions by Vallis and Patla during "burst of air" perturbations could explain movement of the trunk in response to steering via perturbation. As these authors believe, the trunk may be part of a synergy whose direction is dictated by a reference frame defined by the head in the act of steering (Vallis & Patla, 2004). Yet, this egocentric reference frame is also contextually dependent on optic flow and those head and eye movements leading to the change in direction of locomotion (Hollands, Patla, & Vickers, 2002). Even in visuo-locomotor adaptation paradigms, it seems optic flow is the culprit for heading corrections rather than other sensory features such as target drift (Bruggeman, Zosh, & Warren, 2007). Conflicting evidence still exists, however, that suggests motion parallax may play a larger role than optic flow in the control of heading (Schubert, Bohner, Berger, Sprundel, & Duysens, 2003). In sum, visual information is vital to moving the right direction and maintaining the correct heading direction.

Next, there are those studies that investigate how visual information is used to stabilize the head on the trunk during a walking trajectory. When making turns, it has been shown that the head turns approximately 250 ms prior to a shift of the COM in

the medial/lateral plane. Hollands and colleagues suggest that these anticipatory head turns allow the body to reorient itself during turning and are not subservient to gaze (Hollands, Ziavra, & Bronstein, 2004). Additionally, studies by Hicheur and colleagues found that this anticipatory turning of the head has similar orientation angles to both the left and right and could be considered a "global mechanism". They also found that the geometry of the distorted path was reflected in the geometry of the head orientation and noted head rotation was slow in frequency content for stable transfer of body mass (Hicheur, Vieilledent, & Berthoz, 2005). This head and trunk coordination has also been investigated by suppressing the VOR to show a reduced head and trunk coordination that leads to a more stable trunk and less stable head (Cromwell et al., 2004). Finally, having subjects perform tasks with higher gaze stability requirements (reading letters vs. focusing on a dot) increases head instability and did not change trunk stability during locomotion. Introducing the dimension of gaze stability requirements further complicates the stability of the head on the trunk during locomotion (Mulavara & Bloomberg, 2002).

Finding its origins in Gibson's work, the notion that optic flow velocity and displacement may guide locomotion has evolved from sensory phenomena to clinical tool (Gibson, 1958). Being influenced by the moving-room postural studies of Lishman and Lee, Konczak altered optic flow in an experiment where subjects walked in a moving hallway. He found a large portion (42%) of subjects to slow from their regular step velocity when the global optic flow was moving through subjects and a lower portion (25%) of subjects to have faster velocities when the optic flow was moving towards the front of subjects. Konczak proposed the idea that optic

flow velocity does not necessarily destabilize the body; rather, it has a modulatory effect on gait velocity (Konczak, 1994) . Next, Zijlstra and colleagues suggested that visually-guided walking adjusted the ratio of the stride length (SL) over the stride frequency (SF) (Zijlstra, Rutgers, & Van Weerden, 1998). Prokop and colleagues went on to name SL, SF, and walking velocity (WV) the three main components of locomotion in their study of self-driven treadmill walking with tunnel-like virtual display. With their setup, they were able to increase and decrease WV via directional optic flow in a much more efficient manner than Konczak. They found that the SL was changed while SF remained constant during optic flow conditions. Changes in SL, they argue, are the reason that optic flow is able to modulate changes in WV. Also of note, the use of long trial lengths (10 min/~800m) revealed less use of visual information over time as events in the stride cycle increased in variability (Prokop, Schubert, & Berger, 1997) . Last, this guiding effect of optic flow has been shown to aid in the recovery of stroke patients by increasing gait speeds during virtual moving rooms (Lamontagne, Fung, McFadyen, & Faubert, 2007).

In addition to studies that investigate the effects of visual scenes on the velocity of movement, there are studies that investigate the structure of virtual displays and their influence on sway during locomotion. Warren, Kay, and Yilmaz performed a series of experiments with treadmill walking and virtual display that revealed the visual coupling of sway (via neck kinematic) to virtual environment is dependent on the geometry of the scene. In their first experiment, they changed the visual scene by direction (0°, ±30°, ±60°, 90°), type (rotation or translation), and frequency (.25 Hz and .4 Hz). They found similar responses to both rotation and

translation, but much higher responses to the .25 Hz frequency. They also found that sway is directionally specific to driving visual scene. Yet, this directional specificity was anistropic to reveal that visual coupling is higher in the M/L plane than other planes of the body. In their next experiment, they eliminated motion parallax through using a traveling front wall to see if motion parallax was the cause of the anisotropy. They also tested the effect of using varying displacement amplitudes to investigate the "control" of the visual scene. They found that eliminating the traveling hall and using the traveling wall led to a decrease in the anistropic effect while increasing the visual scene displacement caused higher amounts of sway during locomotion until saturation. These higher amounts of sway, however, were not proportional to the increases in visual scene amplitude. In their final experiment, they rotated the platform 90° to change body orientation and made subjects turn their head to the visual scene to test the hypothesis that the anisotropy was due to the constraints of biomechanics or somatosensory stimulation. They found that the anisotropy remained through higher responses in the A/P plane and that this reversal confirmed that the anisotropy was not due to biomechanics or somatosensory input, rather it was due to the distinction between motion parallax and optic flow (Warren, Kay, & Yilmaz, 1996). Not only did this series of experiments support the idea that visual coupling is based on scene geometry, they revealed how sensitive the nervous system is to the many possible changes in visual information.

Indeed, manipulations of visual information have been shown to have an effect on heading, steering, head stability, head-trunk interactions and body sway during locomotion. These studies show that there is a clear need for an investigation

of the degree of which visual information is used to stabilize the body during locomotion. More specifically, what visual manipulations mentioned above positively affect the body's estimation process during locomotion.

Sensory Re-weighting in Posture

During bipedal stance, sensory information is vital to the central nervous system's ability to stabilize the upright configuration of the human body. The body is able to stabilize itself vertical to earth with the regular updating and fusion of visual, somatosensory, and vestibular information. It is well known that intact subjects actively seek out alternative sources of sensory information in destabilizing environments while patients compensate for sensory deficits to stabilize posture (Nashner, 1982). The process of sensory re-weighting (inter-modality) is termed so because of strong coupling of one stimulus with postural sway (up-weighting) in conjunction with weak coupling with another stimulus (down-weighting) (Oie et al., 2002; Peterka, 2002).

Of course, experiments have investigated the interaction of sensory information from vision and surface of support to probe posture for re-weighting capabilities. Sinusoidal anterior-posterior rotations of visual scene during support surface sway referencing to leg angle have shown higher gains to vision up until saturation amplitude of visual scene (Peterka & Benolken, 1995). Additionally, use of the same pseudorandom signal to rotate support surface and visual surround within a trial simultaneously has revealed lower gains of COM in trials where stimuli amplitude increased (Peterka, 2002). Increased velocity of the Center of Pressure (COP) to a visual drive due to sway-referencing the support surface also suggests re-

weighting between these modalities is possible (Mahboobin, Loughlin, Redfern, & Sparto, 2005).

In an experiment investigating the re-weighting of sensory information, simultaneous sensory perturbations of touch and vision in varying amplitudes revealed posture has an intra-modal and inter-modal dependency (Oie et al., 2002). By increasing amplitude of a visual driving signal while keeping a constant amplitude of a touch bar's driving signal (and vice-versa), gains of postural sway to vision (and touch) dropped to reveal intra-modal re-weighting. Additionally, inter-modal re-weighting was observed when gains to vision increased while increasing the amplitude of touch signal only (and vice versa). Observing both inter- and intra-modal re-weighting has been deemed inverse gain re-weighting. Similar interactions have also been observed between support-surface and vestibular sensory inputs (Cenciarini & Peterka, 2006). Indeed, these properties of sensory integration are much more mechanistic than a switch between mutually exclusive sensory drives.

Sensory Re-weighting in Locomotion

An intra-modal sensory re-weighting mechanism utilized in locomotion has not been reported in the literature. However, manipulations of sensory environments that affect two sensory modalities during walking have revealed the potential for inter-modal re-weighting in locomotion. In general, these studies discuss re-weighting on the basis of an output variable showing less of a response to a sensory stimulus due to a disrupting second stimulus.

In studying the interactions of the vestibular and visual systems during goal directed locomotion, Deshpende and Patla found a dynamic weighting of both

systems. In having subjects walk to a target, visual perturbation (prism goggles), vestibular perturbation (GVS-10 second intermittent pulse), or both perturbations were applied. Kinematics of the head and trunk were recorded to yield outcome measures of head and trunk angles as well as displacement from target path. One of the major findings was that vestibular cues were used in the initiation of locomotion (through displacement measures) while the visual cues were used closer to the target. In addition to this functional use of sensory systems, they found the exacerbation of path deviations with ipsi-lateral GVS and prism goggles while contra-lateral stimulations revealed a dominance of vision until GVS actually corrected the path to the target. There were no changes in segment angles across conditions and the authors claim this modulation of target path was due to "dynamic re-weighting of vestibular and visual input" (Deshpande & Patla, 2005). In another study involving young and old subjects, they had similar conditions except for additional amplitude of GVS stimulation. They found that older adults increased their path deviation when the GVS stimulation was doubled while younger adults did not show a similar trend. Additionally, the authors noted the higher head and trunk angle correlation in older subjects (Deshpande & Patla, 2007). Indeed, the literature on re-weighting of the vestibular and visual system is descriptive and could certainly use more fleshing out.

Certainly more mechanistic, a series of experiments by Varraine and colleagues reveals strong evidence for inter-modality re-weighting of somatosensory and visual information in treadmill walking. This group's main concern during walking was the intensity command(IC) which consists of those lower level central pattern generators (CPGs) that will decide the propulsive forces to power through the

gait cycle. As a result, Varraine and colleagues believe maintenance of this IC is the goal of controlling gait. In their first experiment, subjects walked on a self-driven treadmill with backward movement of a virtual hall with the task of maintaining same IC. There were three conditions during this task: FLOW (sinusoidal variations of the optic flow at .0083 Hz), FORC (sinusoidal variations in treadmill resistance at .05 Hz) and COMB (both starting in phase with each other). They found the PSD at the optical perturbation to be greater in COMB condition than in FLOW condition. Also, they found less variation of stride frequency in the FLOW condition than the other two conditions. Finally, they bolstered Prokop's idea of attenuation by finding that the spectrum integral of walking velocity is much lower in the last cycle than the first cycle of gait (Varraine, Bonnard, & Pailhous, 2002).

In a second experiment, Varraine and colleagues told the subjects their goal was to maintain a constant WV in either presence or absence of optic flow and presence or absence of external force perturbation. They found the walking velocity spectrum component in congruent condition lower than condition without optic flow while the force spectrum component is higher with congruent flow than without congruent flow. They reason that compensation for WV changes is in the form of increased force during locomotion. They also note that phase delay in the COMB condition compared to the FLOW represents a neural time delay for integration of force information (Varraine et al., 2002).

Posture and Locomotion: Common use of Visual Information?

Beyond a double support phase and the knowledge that common sensory systems are used, the literature on posture and gait comparisons rarely goes beyond a

biomechanical perspective. Observations like the tendency of forward sway in quiet stance after treadmill walking reveal there is some neural correlate to posture and locomotion in controlling the body, sensing the body, or both (Hashiba, 1998). By using Poincare return maps, Warren and Kay have shown that mode-locking between gait and postural sway reveal that frequency content of gait is altered when stimulus frequency is close to that of the locomotive frequency. Also, they found that higher visual stimulus frequencies cause a higher rate of mode locking of posture and gait. Indeed, a 1:1 mode lock was observed on almost all trials in the frequency range of 0.65 Hz- 0.925 Hz. During this coupling, variability between posture and gait was lower than that of the stimulus with either posture or gait. Warren and Kay also provided a "parametric excitation model" whose results produced similar nonlinear oscillator behavior to the experimental results. Warren and Kay conclude by stating that coordinated systems like gait and posture are the product of a coupled oscillator system (Kay et al., 2001).

Kang and Dingwell, on the other hand, believe that posture and gait are inherently different in terms of dynamic stability. Through use of similar nonlinear analysis mentioned above (see *Dynamic stability*), they were able to define five divergence curve parameters from kinematic recordings of the trunk. By comparing quiet stance and treadmill walking without perturbations, they found significant differences in all of these parameters. As expected, all parameters calculated from walking were significantly larger. Additionally, they attempted to correlate several COP divergence measures to walking and were unable to find any relationship while finding a strong relationship with stance. As these results suggest, they concluded

posture and locomotion were controlled by stabilization processes (Kang & Dingwell, 2006). In the final paragraph of the paper, Kang and Dingwell acknowledge that they have not investigated any actual physiological mechanism that regulates dynamic stability. Moreover, they point out the need for investigations into how physiological mechanisms are different between the tasks of posture and locomotion. These governing mechanisms, they suggest, are different in posture and locomotion. Thus, there exists a need to investigate the body's weighting of sensory information during locomotion in comparison with posture.

Freezing Illusion

As we move through the world, there are the well known perceptions of optic flow and motion parallax. Yet, a sparsely reported and little understood freezing illusion occurs in certain configurations of experiments where either a moving screen or moving subject causes an image on the screen to appear frozen. These studies are reviewed here as this perception may interfere with the availability and/or use of visual information for postural stability during locomotion.

In the first instance of this illusion, Pavard and Berthoz measured the duration of image stabilization while investigating the effects of vestibular stimulation on the perception of visual scene movement (Pavard & Berthoz, 1977). Subjects were sitting in a cart which was accelerated and instructed to push a button when they perceived expanding images in a head mounted display (HMD) to be stabilized. This stabilization time was decreased by decreasing acceleration of the cart, increasing image velocity, increasing the angle of the image relative to the cart, and decreasing spatial frequency of the images. In closing, it was suggested that image velocity is

evaluated with respect to the same static reference frame as the vestibular system rather than being evaluated in reference to the moving subject. Additionally, a model of this illusion was proposed that summarized the stabilization of the images as a visual-vestibular interaction. These authors suggested that this stabilization was a result of an underestimated image velocity due to an increased vestibular sensation over the actual image velocity.

It has also been suggested that this effect is due to an efference copy created from multiple sensory inputs in order to stabilize the world as one moves their body (Probst, Brandt, & Degner, 1986). In a study by Probst and colleagues, seated subjects pushed a button when they detected an oscillating target on a screen in front them to actually move. Detection of this target movement was significantly delayed by increasing frequency of active head oscillations, increasing frequency of head movements with suppression of reactive eye movements, increasing frequency of trunk and leg rotations while the head was fixed in space and increased speed of grating opposite to target motion. The final experiment was most relevant here, as this grating created the perception of self motion as a "yaw-rotation" or circularvection. At the highest interval of this grating speed (60º/s), it took subjects an average of 10.33 seconds to realize the target in front of them was moving. This study shows that manipulating many sensory pathways can reduce the perception of a moving object, and these authors point to neurophysiology to hypothesize that these raised perceptual thresholds are due to self-motion sensation that partially suppresses object-motion detection (Probst et al, 1986).

Also investigating reduced motion perception in seated subjects, Mesland and Wertheim had subjects estimate the relative velocity of a moving grating on a physically moving monitor (Mesland & Wertheim, 1996). In this experiment, subjects sat next to a track on which a TV monitor moved while playing a moving sine-wave grating image. As these subjects fixated on a cross in front of them, their estimates of grating speed were taken after referencing a stationary TV with moving grating. As a result; subjects either reported the grating as frozen on the screen, underestimated the velocity of the grating relative to the monitor, or perceived no change in the grating's velocity relative to the monitor. To separate this study from those previously mentioned, this freezing of the grating occurred without any movement (passive or active) on behalf of the subject and had a cause that was certainly visual (Mesland & Wertheim, 1995). A mathematical model was later developed based upon this experiment to explain this "freezing effect" and reduced perception in scene motion (Wertheim & Reymond, 2007). Central to this model, a just noticeable difference (JND) term must be eclipsed by the sum of the velocity of a reference signal and velocity of the stimulus on the retina in order to perceive velocity of the stimulus. These authors' description of the JND includes neural noise while this reference signal is the sum of the efference copy and ego-motion (Wertheim & Reymond, 2007).

As all of these studies have dealt with seated subjects, there are few studies that have investigated the reduced perception of scene motion during actual walking. In a study where subjects walked on a treadmill at different speeds in front of an optic flow display, subjects underestimated optic flow velocity more as speed increased

(Thurrell, Pelah, & Distler, 1998).Furthermore, this reduction in image velocity estimation is weaker with less natural scenes such as translating gratings or rotating wheels when compared to optic flow (Thurrell & Pelah, 2002). Durgin and colleagues would later suggest an extension of Barlow's (1990) theory of sensory inhibition in a "multicue subtractive model" to explain reductions in perceived speed of optic flow during locomotion. The support for this hypothesis came from an experiment where subjects reported the perceived speed of optic flow in an HMD while being pushed on a cart (passive motion with translation), walking on a treadmill (active motion without translation), and walking over ground (active motion with translation). Indeed, the sum of reductions in perceived speed during passive motion and reductions in perceived speed during treadmill walking approximated that of over-ground walking. These authors argued that perceived reductions in flow speed while walking are due to self-motion estimates by both motor and vestibular system to confirm their "multicue subtractive model" (Durgin, Gigone, & Scott, 2005).

Chapter 3: Pilot Investigation

In an initial pilot investigation, a sum of sines stimulus was used to probe responses to a translating visual scene in three subjects. The purpose of this pilot study was to test the possibility of detecting kinematic responses at several frequencies of visual input.

Methods

Three healthy adults from the university setting consisting of one female and two males were used in this pilot study. All subjects were self reported to have no history of balance disorders or dementia, and were not using prescription drugs that affect balance. Additionally, subjects had no history of surgical procedures involving the feet, ankles, knees, hips, back, brain, spinal cord or inner ear.

Apparatus

Virtual Display and Treadmill. Subjects stood or walked on a treadmill (EN-MILL 3446.527, Bonte Zwolle BV, The Netherlands) at different controlled speeds (0, 1, 3, 5 km/h). The treadmill was positioned in front of a 4m x 4m rear-projection screen that encompassed the field of vision. The visual display consisted of 500 randomly-distributed white triangles (3.4 cm/side) on a black background, updated at 60 Hz. The display translated a sum of sines signal in the A/P plane at approximately the subject's eye height. This sum-of-sines signal contained ten sine waves with the following frequencies:

$$f(i)=(.024, .056 , .104 ,.184 ,.344 ,.584 ,.904 , 1.432, 2.104, 2.936)$$

Amplitude (A) was equal to .08 deg Hz. Amplitudes of successive frequency (i) were scaled in the following manner: if $i < 8$, $A_i = A/f_i$ and if $i > 8$, $A_i = A/f_8$.

Kinematics. Kinematic data were recorded bilaterally at 100 Hz by means of the Vicon-612 system (Oxford, UK) with nine television cameras spaced around the walkway. Infrared reflective markers (diameter 1.4 cm) were attached bilaterally to the skin overlying the following landmarks: gleno-humeral joint (GH), the midpoint between the anterior and the posterior superior iliac spine (ilium, IL), greater trochanter (GT), lateral femur epicondyle (LE), lateral malleolus (LM), heel (HE), and fifth metatarso-phalangeal joint (VM). Reflective markers were also placed at the occipital, left temple and right temple locations of the head. For two subjects, reflective markers were also placed at L1 and T1.

Procedures

Subjects walked with their shoes on and were asked to swing their arms normally and to look straight ahead. Before the recording session, subjects practiced for a few minutes in walking and running on the treadmill at different speeds. All subjects were given the same oral instructions. Four trials of each treadmill speed were attempted for 125 seconds using the same visual stimulus. Trials were thrown out if more than ¼ second of consecutive data were not recorded by motion capture system.

Subject	0(Posture)	1 km/h	3 km/h	5 km/h
ND	3	4	4	3
JJ	3	4	4	2
YI	4	4	3	4

Table 3.1. Successful Trials in Pilot Study

Analysis

Due to difficulties with capturing kinematic data, several of these anatomical markers went missing to cause exclusion from data set all together. With the assumption of symmetry, we look at unilateral data on the left side. The results include the following analysis on the joint displacements in the A/P plane of the left ankle, knee, hip, and shoulder. Additionally, it includes the back of head, T1 and L1.

Spectral Analysis. For each trial, joint displacements were "demeaned" and power spectral densities (PSDs) of stimulus and joint displacements were calculated and cross spectral density (CSD) between the stimulus and joint displacement were computed in Matlab using Welch's method with a Hanning window and 50% overlap. The window size used at each frequency was the closest multiple of that frequency near 20 seconds. This was performed to prevent the inflation of coherence measures.

Gait Frequency. Frequency of gait was calculated at each speed by calculating shank segment (knee to ankle) elevation angles and then computing PSDs on trial basis in the same manner.

Complex Coherence: Magnitude Squared Coherence and Phase. For each subject and condition, complex coherence was calculated as $C_{12}=P_{12}/ (P_{11}*P_{22})^{1/2}$. Magnitude squared coherence is the absolute value squared of this value while the Phase is the argument of C_{12}.

Gain and Phase. The outcome measures used to characterize FRFs of kinematics from stimuli were gain and phase. Gain is the absolute value of the FRF at the stimulus frequency. Unity gain indicates that the anatomical point's amplitude at the stimulus frequency exactly matches the amplitude of the sensory stimulus. Phase, the argument of the FRF, indicates the temporal relationship between the anatomical

point and the sensory stimulus and body sway, and was defined as the angle of the FRF at the stimulus frequency. A phase lead is indicative of anatomical point being temporally ahead of a sensory stimulus (and vice versa for phase lags).

Preliminary Findings

The time series of AP displacement in a single trial reveal typical movements of the joints in conditions investigated (Fig. 3.1). During the standing posture condition, the knee and ankle appeared relatively immobile while the rest of the kinematic markers show similar movement about the AP plane.

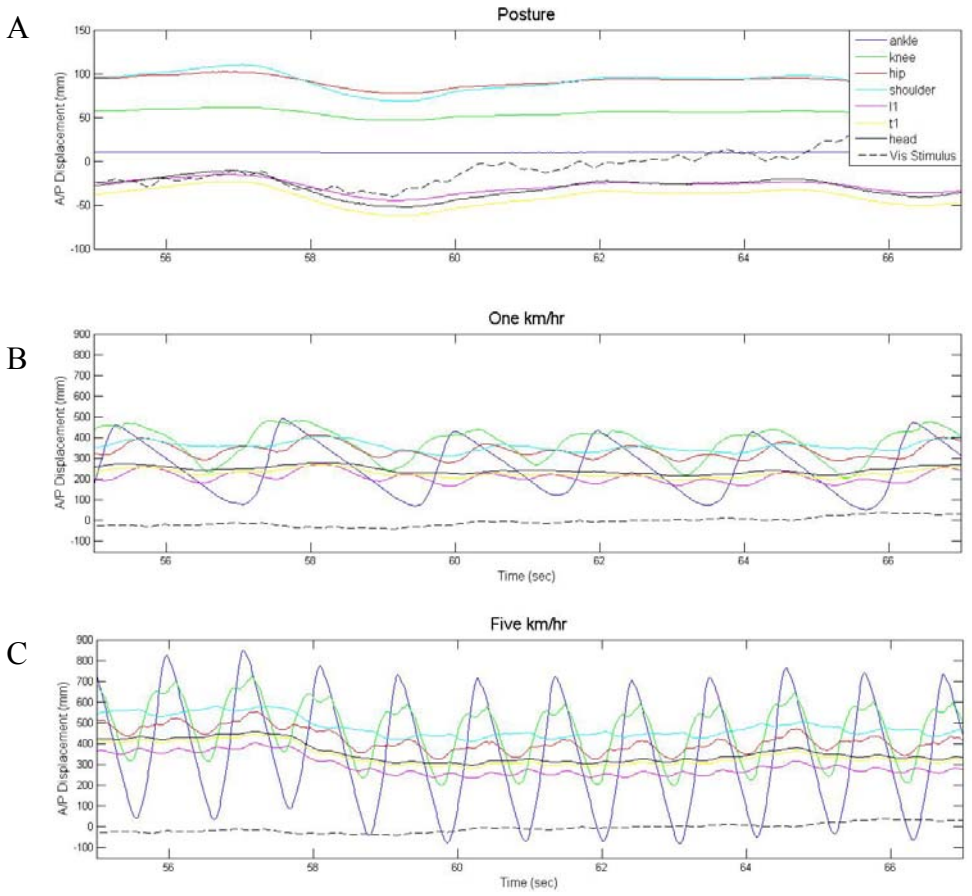

Figure 3.1. Time Series of AP Displacement. A: Single trial of subject "JJ" in standing posture during translating visual scene. B: Single trial of subject "JJ" in one km/hr treadmill movement during translating visual scene. C: Single trial of subject "JJ" in five km/hr treadmill movement during translating visual scene. Positive implies forward of the body while negative is backwards.

Moving from one km/hr to five km/hr, oscillatory motions of the joints become more prevalent in all subjects. Starting in the one km/hr condition, noticeable oscillation in the knee and ankle occurs and increases in amplitude occur as treadmill speed is increased. Most noticeable in the five km/hr condition, the ankle, knee, and hip are in-phase with characteristic waves based on joint motion. Also noticeable in this condition, the back of the head oscillates at twice the frequency of these points on the lower body (Fig. 3.1C).

Power Spectral Density and Locomotive Frequency

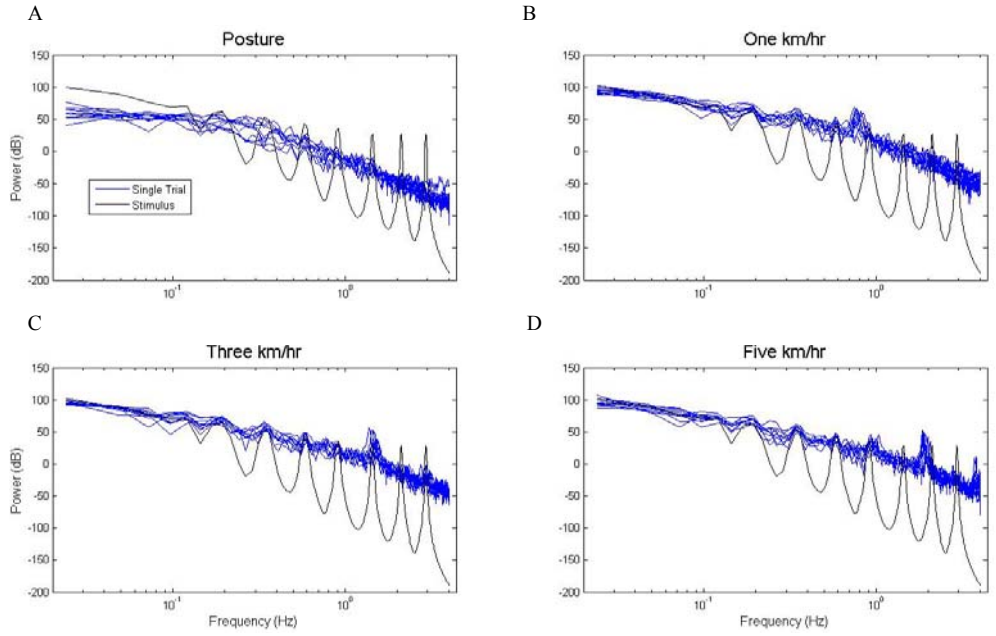

Figure 3.2. PSDs of Head. A-D: Power Spectral Densities (PSDs) of A/P head displacement in posture, one km/hr, three km/hr and five km/hr. Each blue line is a single trial of that condition to include all trials of all subjects. The PSD of the sum of sines stimulus (black) is also included (n=3).

Due to its generally high gain to the visual stimulus, power spectral densities (PSDs) of the AP head displacement are presented (Fig. 3.2). Plotting every trial's PSD from every subject (blue lines) with stimulus PSD (black) reveals a consistent

spectral pattern across subjects. As typical of the kinematics above the trunk for these three subjects, the coupling of PSD peaks is not so clear in the postural condition

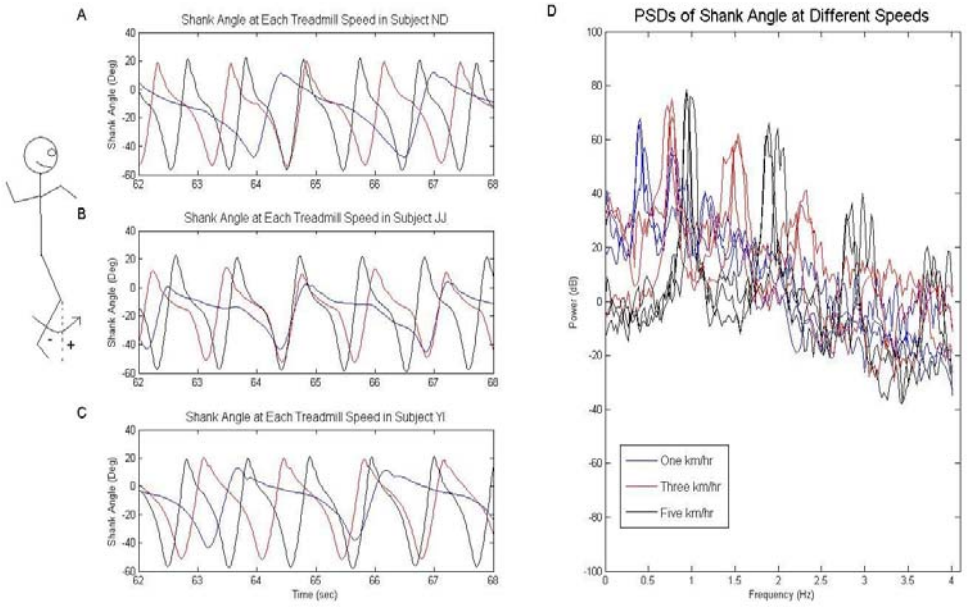

Figure 3.3. Locomotion Frequency. A-C: Shank Angles to elevation in A/P plane for all three subjects in one, three, and five km/hr conditions in the middle of a single trial. D: Subject averages of power spectral density (PSD) of the shank angle in one, three, and five km/hr conditions. Each line represents a single subject's average shank angle PSD for that condition (n=3).

while the treadmill speed conditions reveal coupling of the head to the visual drive. The middle range of stimulus frequencies, however, show very strong coupling in treadmill conditions. As the treadmill speed increases, it seems the response across subjects is less variable at stimulus peaks. Obviously, this trend is clearer in the difference between the one km/hr and five km/hr condition than the one km/hr and three km/hr condition. There also seems to be a broad, locomotive peak that moves along the x-axis as speed increases (Fig. 3.2B-D).

To investigate this locomotive peak further, shank angles were calculated for all trials of all subjects. These angles show similar trends in range of deviation and

general overall pattern to reveal common knee extension to elevation angle (~ +20°) and knee flexion (~ -55°) in the five km/hr condition (Fig. 3.3A-C). As expected, this range of motion was smaller in slower treadmill speed conditions. PSDs of these shank angles reveal the locomotive frequency during each treadmill condition (Fig. 3.3D). These PSDs are subject averages for each condition and reveal spectral power of the shank angle for the one km/hr to be in the .5-.55 Hz frequency range, three

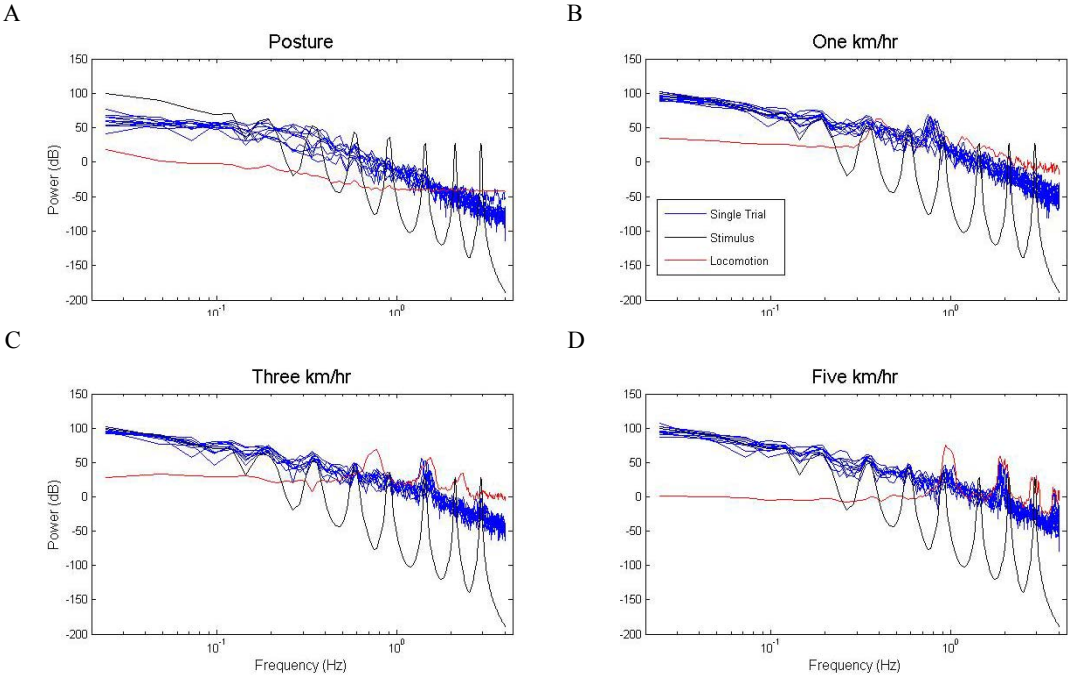

Figure 3.4. PSDs of Head with Locomotion Frequency. A-D: Power Spectral Densities (PSDs) of A/P head displacement in posture, one km/hr, three km/hr and five km/hr. Each blue line is a single trial of that condition to include all trials of all subjects. The PSD of the sum of sines stimulus (black) and the across-subjects mean of locomotive frequencies computed in Fig. 4 are also included (red, n=3).

km/hr to be in the .8-.85 Hz frequency range, and five km/hr condition to be in the 1.05-1.10 Hz frequency range. Resonant peaks are also present at the corresponding multiples of these frequency ranges. Finally, the across subject averages of these locomotive frequencies are plotted on Figure 3.2 to show the frequency of locomotion

at the head (Fig. 3.4). The PSDs of head AP displacement align with first resonance frequency of the locomotive frequency (red) during the treadmill conditions.

Complex Coherence

The squared, real portion of the complex coherence reveals a change in linear relationship between AP displacement of the joints and vision due to treadmill condition. In posture, this measure fluctuates around .1 up until above 1 Hz and drops dramatically afterwards. In the one km/hr condition, this coherence is higher and similar across joints until .1 Hz when ankle and knee coherence dip drastically to fluctuate in the remaining frequencies. Kinematics at the hip and above, however, share similar coherence patterns until about .5 Hz when the hip remains higher than all other kinematics until 1.4 Hz. During the three km/hr condition, coherences for all joints are at a similar magnitude up until the .3 Hz frequency stimulus. Ankle, knee, and hip coherences dip drastically after this frequency while hip recovers in later frequencies. Yet, the rest of the joints remain in unison until spreading apart at about 1 Hz. The split in coherence during the five km/hr condition is seen at the .5 Hz stimulus frequency with coherence at the ankle beginning its drop in the prior stimulus frequency. The shoulder, knee, and ankle coherence drop together while the rest of the kinematics pattern together for most of the remaining frequencies.

The phase of the complex coherence between AP displacement of kinematics and vision also changes as the treadmill condition changes. In the standing posture condition, phase leads were generally observed until .1 Hz. Afterwards, a common decline in phase was seen until .5 Hz where these phases split into a less-lagging group of the head,t1 and shoulder and more-lagging group of the rest of the

kinematics. Next, phases during the one km/hr condition revealed a phase lead for all kinematics up to .1 Hz where the ankle became drastically different from the rest of the body. Phases of the rest of kinematics generally lagged together until the .9 Hz where most split from each other. In the three km/hr condition, however, phases of kinematics led together until crossing at .1 Hz to lag together until about .5 Hz when phases spread apart. Finally, phases of kinematics in the five km/hr condition showed a phase lead together until crossing at .1 Hz to lag together until about .9 Hz when phases spread apart drastically.

Gain and Phase

For the most part, trends in gains of the kinematics to the translating visual scene mimic those of the coherence. Low compared to other conditions, gains in standing posture increase until about .3 Hz and then decline in the remaining frequencies. Gains of the ankle to the visual scene are an order of magnitude lower than the other anatomical points (Fig. 3.5A). In the one km/hr condition, gains of all kinematics increased together in the low frequencies up to .1 Hz except the hip whose peak gain was at .3 Hz. Afterwards, the ankle gain dropped more than other kinematics to drastically rise again at 2.1 Hz. For the most part, these other kinematics decreased in the remaining frequencies. During the three km/hr condition, gains increase up to .1 Hz for the shoulder, head and t1 while the other kinematics rise until .3 Hz. After .3 Hz, gains of the knee and ankle fluctuate drastically to finding a maximum gain at 2.1 Hz. Interestingly, gains of hip and l1 fluctuate in opposite directions after .5 Hz while shoulder, head and t1 decline together from .1Hz.

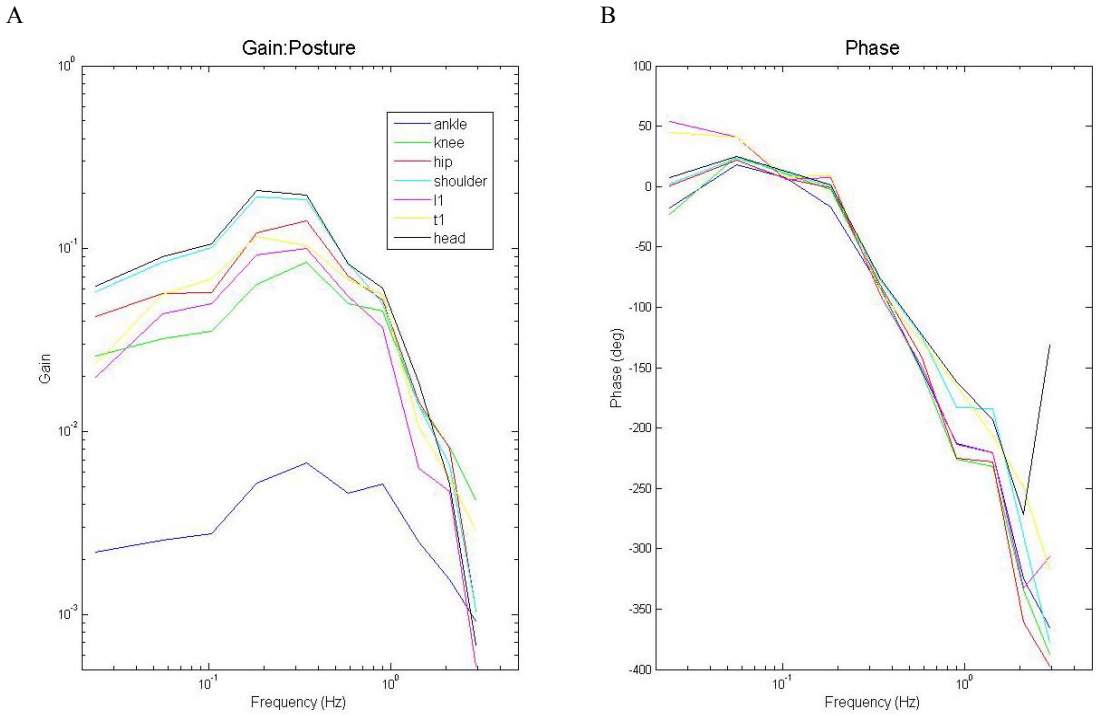

Figure 3.5. Mean FRF: Posture. A: Gain of A/P displacement of anatomical markers with visual stimulus signal during standing posture. B: Phase of A/P displacement with visual stimulus in standing posture (n=3).

And in the five km/hr condition, the gains of all kinematics have similar trends up to .5 Hz. After .5 Hz, the head, l1, and shoulder show a declining relationship to the visual scene. The ankle, knee, and hip fluctuate in the remaining frequencies to have their maximum gains at 1.4 Hz. L1, however, declines until resurging in gain with the ankle, knee, and hip at the 2.1 Hz stimulus frequency (Fig. 3.6A).

Phase relationships of the FRFs from translating visual scene to body kinematics also change across locomotion conditions. At the lowest frequency of stimulation in the standing posture condition, only knee and ankle lag the stimulus while the remaining kinematics lead the stimulus. After this frequency and prior to the .18 Hz stimulus, all kinematics are behaving similarly and leading the stimulus

until after .18 Hz. Lagging together until .5 Hz, the kinematics split and shoulder, l1, and head lead the other kinematics (Fig. 3.5B).During the one km/hr condition, all kinematics lead the stimulus until crossing over 0° at the .18 Hz stimulus. After this

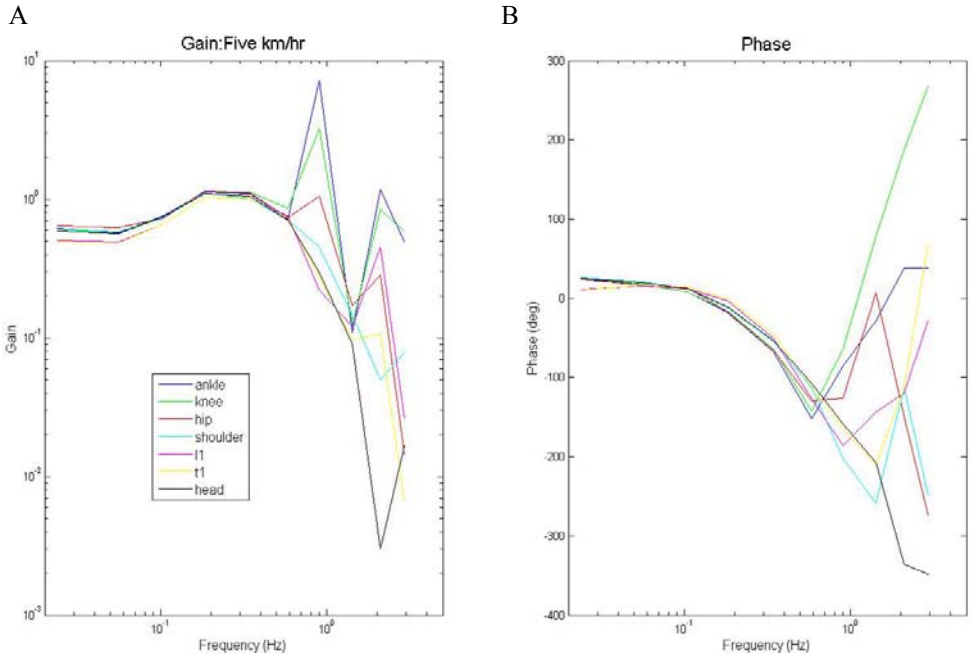

Figure 3.6. Mean FRF: Five km/hr. A: Gain of A/P displacement of anatomical markers with visual stimulus signal during five km/hr treadmill motion. B: Phase of A/P displacement with visual stimulus in five km/hr treadmill motion (n=3).

frequency, all kinematics lag in the remaining frequencies. However, the phases of the ankle, knee and hip seem to lead the other kinematics at higher frequencies. Next, the three km/hr condition yields similar leading and lagging behavior as the one km/hr condition. In this condition, all kinematics lag the stimulus together until .5 Hz. Afterwards, phase behavior is quite erratic across kinematics. Lastly, phase behavior in the five km/hr condition is almost identical to the phase relationship between kinematics and visual stimulus found in the three km/hr condition (Fig. 3.6B).

Chapter 4: Intra-modal Reweighting

As a result of the pilot investigation, it was determined that similar methods of probing sensory integration in posture may be applied to locomotion at a wide range of frequencies. To address hypotheses 1-3; responses of twelve subjects were measured during broad-band visual scene motion at a low and high amplitude in posture, one km/h, and five km/h.

Methods

Subjects

Twelve healthy subjects [5 males and 7 females, between 20 and 31 yrs of age, 69.4 ± 16.2 kg] received financial compensation for participating in this study. All subjects were self reported to have no history of balance disorders or dementia, and were not using prescription drugs that affect balance. Additionally, subjects had no history of surgical procedures involving the feet, ankles, knees, hips, back, brain, spinal cord or inner ear. The studies conformed to the Declaration of Helsinki, and informed consent was obtained from all participants according to the procedures of the Ethics Committee of the Santa Lucia Institute.

Apparatus

Virtual reality environment. Subjects walked or stood on a treadmill (EN-TRED 1475.911, Enraf-Nonius, Netherlands) one meter in front of a translucent screen (4x4m) with a rear-projected virtual display with dimensions 2.55 m wide by 1.82 m high at position 0**,** as shown in Figure 4.1**.** Subjects wore goggles with occluded sides to prevent them from seeing the border of the visual display, which consisted of 500 randomly-distributed white triangles (2.6 x 2.6 x 2.4 cm) on a black

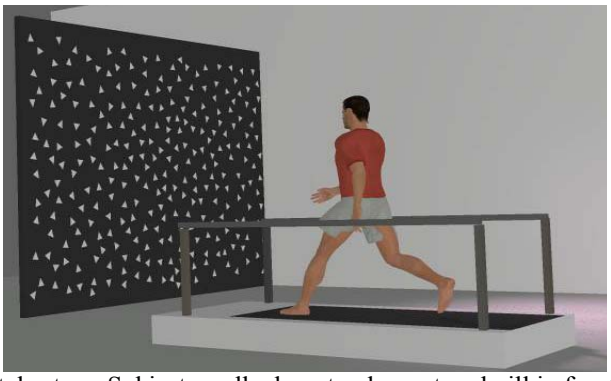

Figure 4.1. Experimental setup. Subjects walked or stood on a treadmill in front of a projection screen with a rear-projected virtual display. Subjects wore goggles with occluded sides to prevent them from seeing the display's border. This display consisted of 500 randomly-distributed white triangles on a black background.

background, updated at 60 Hz. The virtual display was created using CaveLib software (Mechdyne, USA) with projection through a digital projector (MP3135, HP,USA) synched to a desktop computer (Precision PWS490, Dell, USA). Visual signals were created offline (Matlab, Mathworks, USA) and generated via Labview (National Instruments, USA) on a desktop computer (Pentium 4, HP, USA).

Visual scene signals. These driving visual signals were either a high or low amplitude filtered white noise signal that translated in the sagittal plane. For each trial of each subject, a different seed was used to generate a white noise signal using a random number generator. High amplitude signals had a one-sided spectral density of 156.8 cm^2/Hz while low amplitude signals had a spectral density of 9.8 cm^2/Hz, as shown in Figure 4.2. These signals were then filtered using a first-order Butterworth low-pass filter with a cutoff of .02 Hz and an eighth-order Butterworth low-pass filter of 5 Hz. In doing so, power of scene motion was concentrated in lower frequencies where postural responses to sensory inputs are known to occur. Across subjects and speeds, the high amplitude signal had an average RMSE of 1.989 cm and 3.499 cm/s while the low amplitude signal had an average RMSE.523 cm and .878 cm/s. A

positive/negative signal corresponded to an anterior/posterior translation. A one cm negative translation of the visual scene corresponded to an expansion of the triangles to 3.4 x 3.4 x 3.2 cm. Visual display generation and data collection software were synchronized via an external trigger.

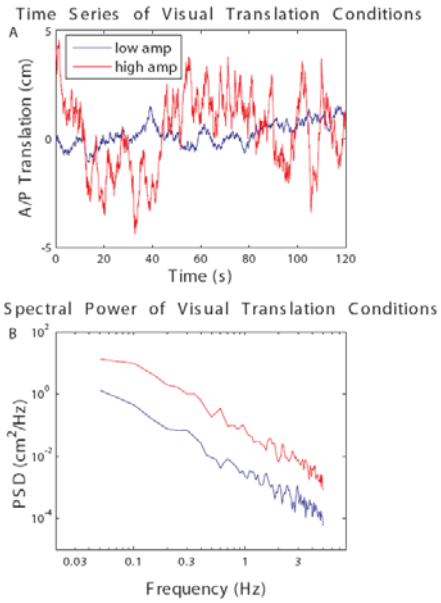

Figure 4.2. Stimuli. A: Example time series of low and high amplitude signals used. Positive deviations corresponded to A/P translation of virtual scene into screen while negative deviations corresponded to translation out of screen towards subject. B: One sided PSDs of these signals up to 5 Hz.

Kinematics. Body kinematics were measured using a VICON motion capture system (VICON,Inc, Oxford, UK). Reflective markers were placed on the right and left sides of the body at each of the following landmarks: the base of the 5th metatarsal, the posterior calcaneus (heel), the lateral malleolus (ankle), the lateral femoral condyle (knee), the greater trochanter (hip), and the acromion process (shoulder). Additionally, a marker was placed at the center of the back of the head. Segment angles from vertical were computed for the foot, shank, thigh, leg and segment on each side of the body. All kinematic data were collected at 100 Hz

Procedures

Prior to experimentation, subjects experienced a static visual display at the experimental locomotion speeds. Subjects began each experimental trial by looking straight ahead at the visual display screen. Once they were ready, subjects said "Go" and the experimenter initiated treadmill movement for approximately 30 seconds for the subject to reach steady-state. At this point, the subject would declare if he or she was ready for the trial to begin. The experimenter then initiated data acquisition/scene translation with variable delays to avoid start-up effects. Each trial was 120 seconds in duration with a rest of 60 seconds in between trials. One subject had 3 trials per condition, while 16 trials were discarded for other subjects due to a missing kinematic for that trial. The experimental design consisted of two amplitudes of visual scene motion (low-high) and three treadmill speeds (0, 1, 5 km/hr) for a total of six conditions.

Analysis

Frequency response functions: gain and phase. Measures of gain and phase were computed from the frequency response functions (FRFs) of the A/P translation of shoulder, hip and approximate trunk angle to visual scene motion. First, Fourier transforms of the de-meaned visual scene translations ($x(t)$) and these de-meaned kinematics ($y(t)$) were calculated. One-sided power spectral densities (PSDs) and cross spectral densities (CSDs) using Welch's method with a 20 second Hanning window and one-half overlap were then calculated with these transforms. These PSDs and CSDs were then averaged within condition for each subject. For each subject, PSDs and CSDs of stimulus frequencies up to 3.7 Hz were binned linearly on a logarithmic scale to create ten frequency bins. Stimulus frequencies in the following

ranges created the ten bins: .05, .1, .15, .2-.3, .35-.45, .5-.7, .75-1.1, 1.15-1.65, 1.7-2.5, and 2.55-3.7 Hz. For plotting purposes, binning these stimulus frequencies yielded bin averages of .05, .1, .15, .25, .4, .6, .925, 1.4, 2.1 and 3.125 Hz.

Using these binned PSDs and CSDs, complex coherence was calculated as $c_{xy}(f) = P_{xy}(f)/\sqrt{P_{xx}(f)P_{yy}(f)}$. Across subjects, the FRF was defined as $\bar{H}_{xy}(f) = \bar{c}_{xy}(f)\sqrt{\bar{P}_{yy}(f)/\bar{P}_{xx}(f)}$ where $\bar{c}_{xy}(f)$ is the mean complex coherence and $\bar{P}_{yy}(f)$ and $\bar{P}_{xx}(f)$ are geometric mean PSDs (Kiemel et al., 2008). Although this method weights subjects with higher coherences in each bin, we believe this method is suitable as it is common place in similar studies (Warren et al, 1996, Kay and Warren, 2001) to analyze those results found from responders when subjects are initially divided into those whose movements are affected by visual scene motion and those who are not.

The outcome measures used to characterize these FRFs were gain and phase. Gain is the absolute value of $\bar{H}_{xy}(f)$ and phase is the argument of $\bar{H}_{xy}(f)$, converted to degrees. A gain of one indicates a proportional response of $y(t)$ to $x(t)$ while a positive phase indicates that $y(t)$ was phase advanced relative to $x(t)$.

Normalized FRFs. To investigate the effects of the gait cycle on the calculation of these FRFs, a multiple of the average gait period in each trial was used as the size of the spectral window. Gait period for each trial was the average length of time between toe-off events, which were identified from leg axis minima. The leg axis minima were defined as the local minima of the angle formed by the fifth metatarsal-hip axis in the sagittal plane. FRFs were computed in the same manner as above with

the only caveat being that the spectral window for each trial was ten multiplied by the average gait period for each trial.

Statistics

Due to our probe of a relatively wide band of frequencies, initial statistical tests for FRFs were determining if lower bounds on gain in each bin of each condition were greater than zero. First, 95% confidence intervals for log gain and phase of these FRFs were computed using the bootstrap percentile-*t* method with 4000 bootstrap resamplings and 400 nested bootstrap resamplings for variance estimation (Zoubir & Boashash, 1998). These FRFs were considered real, with gain greater than zero, when this confidence region was different from 0 in the complex plane (α=.05).Log gain and phase are plotted with error bars representing ± standard deviation of 10,000 bootstrapped resamplings using the percentile t-method (Zoubir & Boashash, 1998).

To compare log gain and phase between amplitude, speed, and kinematic output; 95% bootstrap confidence intervals were computed for differences in log gain and differences in phase. Interaction effects were identified by computing differences of these log gain differences and phase differences. Differences in gain and phase were found when these confidence intervals did not include one and zero, respectively. Changes in log gain and phase are illustrated by plotting mean gain ratios and phase differences with their 95% confidence intervals.

Results

Gain and Phase: Displacements

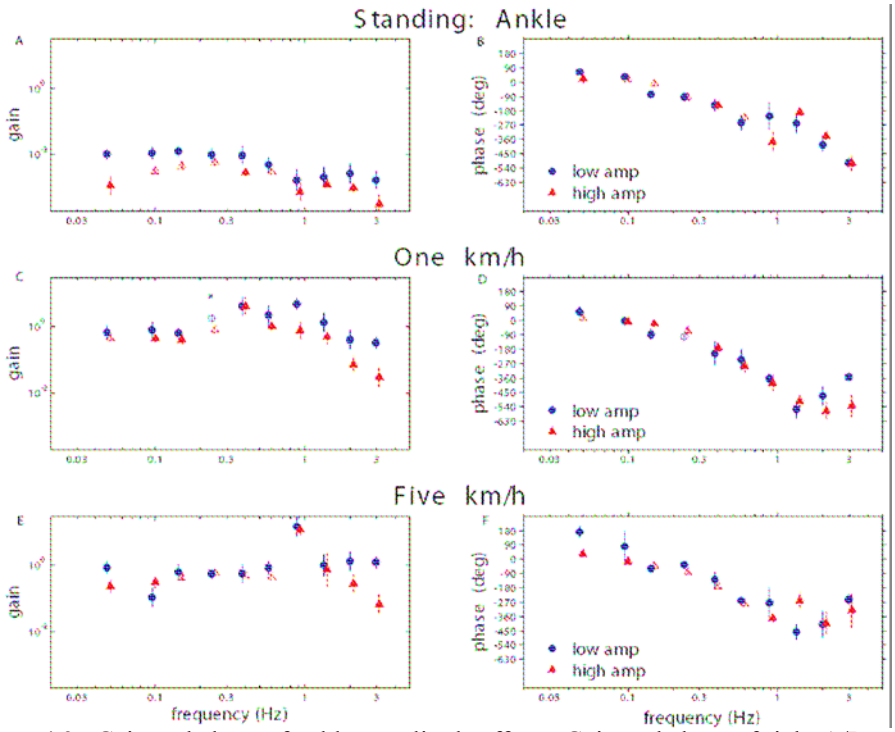

Figure 4.3. Gain and phase of ankle: amplitude effects. Gain and phase of right A/P ankle displacement with visual scene motion in each condition. Open face symbols represent those frequency bins where gains were different from zero. Asterisks represent significant, real differences in amplitude (α=.05). Error bars are bootstrapped standard error (n=12).

Figures 4.3-.6 show gain and phase of displacements of ankle, knee, hip and shoulder on right side of the body. Open face symbols represent those frequency bins where initial tests of significance reveal that these responses of gain and phase can be considered real (α=.05). These figures are representative of the trends in the transfer functions computed for responses of displacement. Initial tests of significance revealed gain was different from zero in a small number of frequency bins for fifth metatarsal, ankle, heel, knee, hip and shoulder in low amplitude conditions (standing-8/60; 1 km/hr - 7/60; 5 km/hr – 2/60, α=.05). Likewise, initial statistics on the left side of the body in low amplitude conditions show few differences from zero(standing-8/60; 1 km/hr - 1/60; 5 km/hr – 5/60, α=.05). As for high amplitude

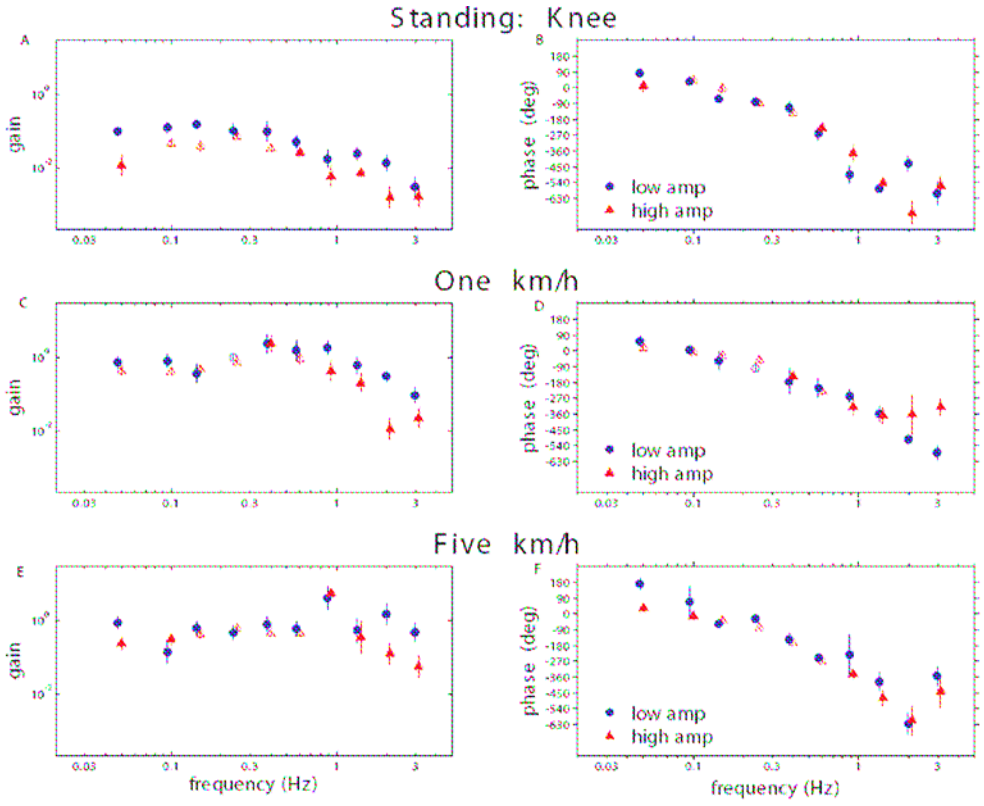

Figure 4.4. Gain and phase of Knee: amplitude effects. Gain and phase of right A/P knee displacement with visual scene motion in each condition. Open face symbols represent those frequency bins where gains were different from zero. Asterisks represent significant, real differences in amplitude (α=.05). Error bars are bootstrapped standard error (n=12).

conditions, there are much more consistent responses when looking at these single side transfer functions. Responses in both the right side of the body (standing-27/60; 1 km/hr - 18/60; 5 km/hr – 24/60, α=.05) and the left side of the body (standing-23/60; 1 km/hr - 17/60; 5 km/hr – 25/60, α=.05) are more consistent in posture and 5 km/h conditions.

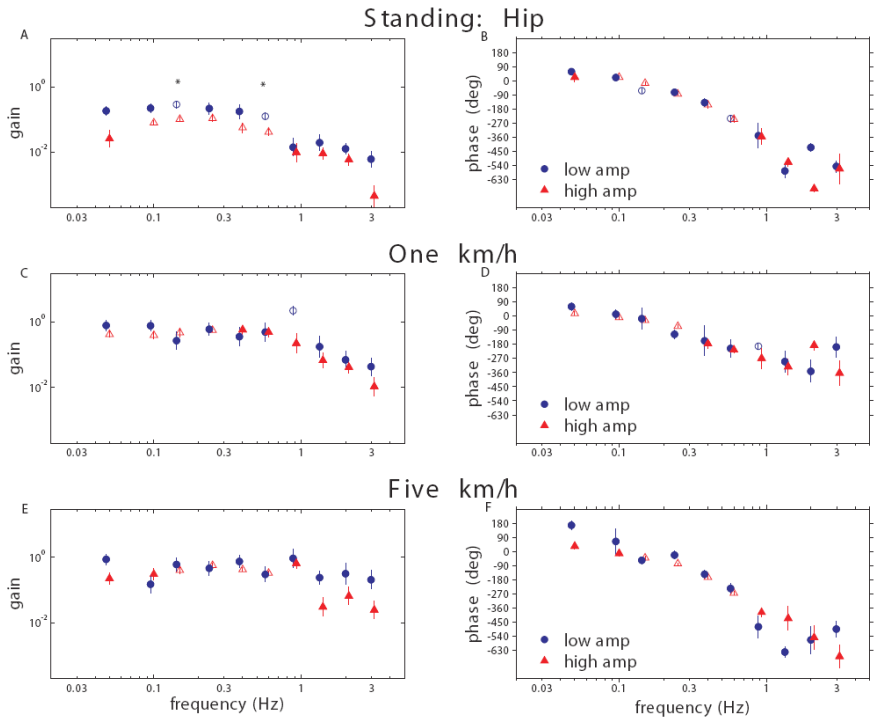

Figure 4.5. Gain and phase of Hip: amplitude effects. Gain and phase of right A/P hip displacement with visual scene motion in each condition. Open face symbols represent those frequency bins where gains were different from zero. Asterisks represent significant, real differences in amplitude (α=.05). Error bars are bootstrapped standard error (n=12).

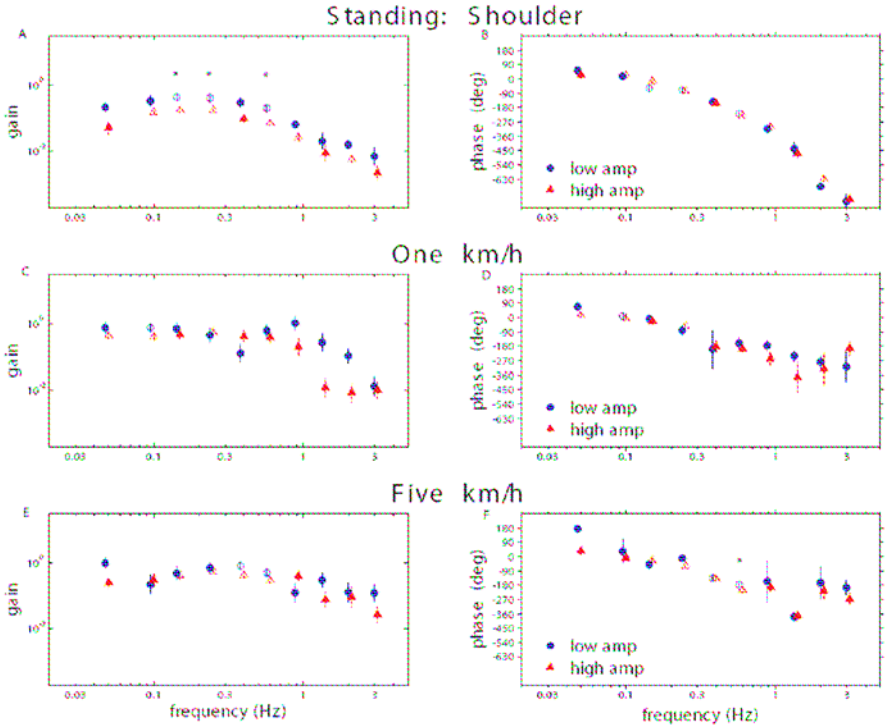

Figure 4.6. Gain and phase of Shoulder: amplitude effects. Gain and phase of right A/P shoulder displacement with visual scene motion in each condition. Open face symbols represent those frequency bins where gains were different from zero. Asterisks represent significant, real differences in amplitude (α=.05). Error bars are bootstrapped standard error (n=12).

As can be gathered these figures, there are very few instances where both low and high amplitude responses to visual scene motion at the same speed are real in the same bin. In cases where amplitude dependent changes in gain were testable; 7/8 had significant amplitude dependent changes in gain in posture, 4/6 in one km/h, and 0/6 in five km/h in both sides of the body. In all of these cases where amplitude dependent changes in gain occurred, gains of kinematics to visual scene motion were higher in the low amplitude condition than the high amplitude condition. For posture conditions, all of the amplitude dependent changes in occurred in either hip or shoulder responses. As Figures 4.5-.6 reveal, 5/7 changes in gain during standing posture were due to the right hip in bins 3 and 6 as well as the right shoulder in bins 3-4 and 6. The other changes in gain occurring in posture occurred at bin 2 in the left hip and bin 6 in the left shoulder. Interestingly, 3/4 amplitude dependent changes in gain that occurred at one km/h occurred at the three markers on the right foot at frequency bin 4. Figure 4.3C shows the decrease in the ankle's response to vision at bin 4. Finally, 4/6 cases where changes in gain could be tested at 5 km/h were at either a hip or shoulder marker. Indeed, this is evidence that amplitude dependent changes in gain did not occur in the trunk when possible at 5 km/h.

As amplitude dependent changes in gain did not occur in the same marker and bin at different speeds, interactions of amplitude and speed cannot be tested. For similar reasons, testing which portions of the body (lower vs. upper, etc.) show larger amplitude dependent changes in gain cannot be determined.

Gain and Phase: Segment Angles

Figures 4.7-.8 show gain and phase of leg and trunk angles on the right side of the body. Once again, open face symbols represent those frequency bins where initial tests of significance reveal that these responses of gain and phase can be considered real (α=.05). Similar to displacements, initial tests of significance revealed gain was

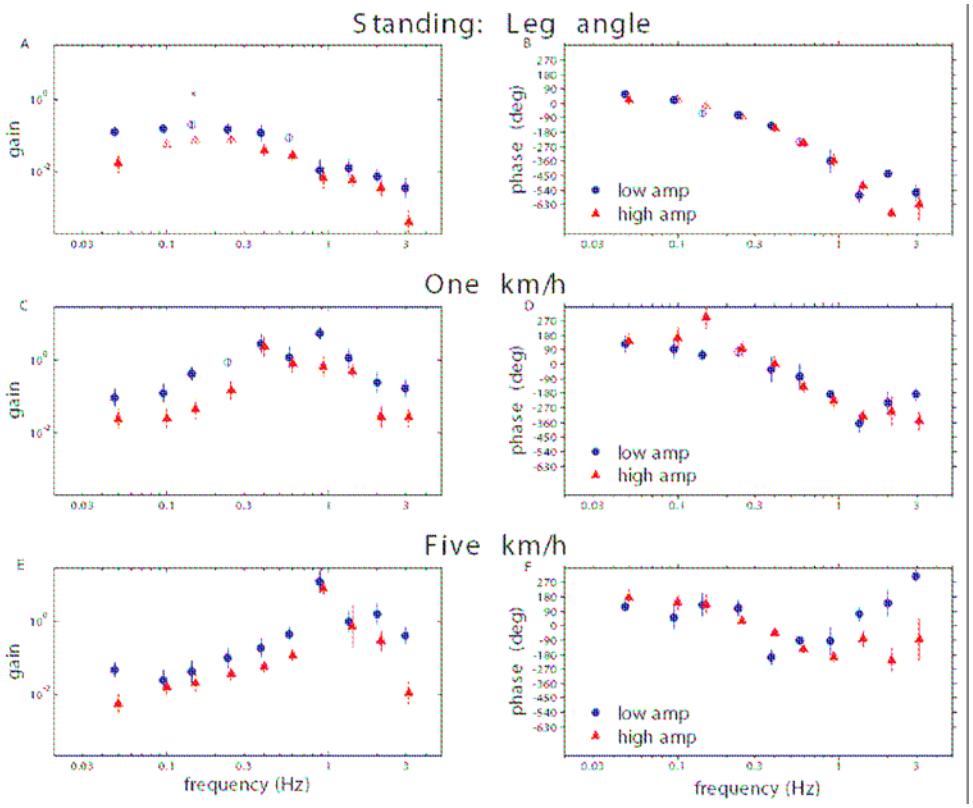

Figure 4.7. Gain and phase of leg angle: amplitude effects. Gain and phase of right leg angle with visual scene motion in each condition. Open face symbols represent those frequency bins where gains were different from zero. Asterisks represent significant, real differences in amplitude (α=.05). Error bars are bootstrapped standard error (n=12).

different from zero in a small number of frequency bins for foot, shank, thigh, leg and trunk in low amplitude conditions (standing-8/50; 1 km/hr - 1/50; 5 km/hr – 2/50, α=.05). Also, initial statistics on the left side of the body in low amplitude conditions show few differences from zero (standing-11/50; 1 km/hr - 5/50; 5 km/hr – 0/50, α=.05). Unlike displacements, responses of segment angles for the right (standing-20/50; 1 km/hr - 2/50; 5 km/hr – 5/50, α=.05) and left (standing-20/50; 1 km/hr -

1/50; 5 km/hr – 4/50, α=.05) sides of the body did not become more consistent in high amplitude compared to low amplitude conditions during locomotion.

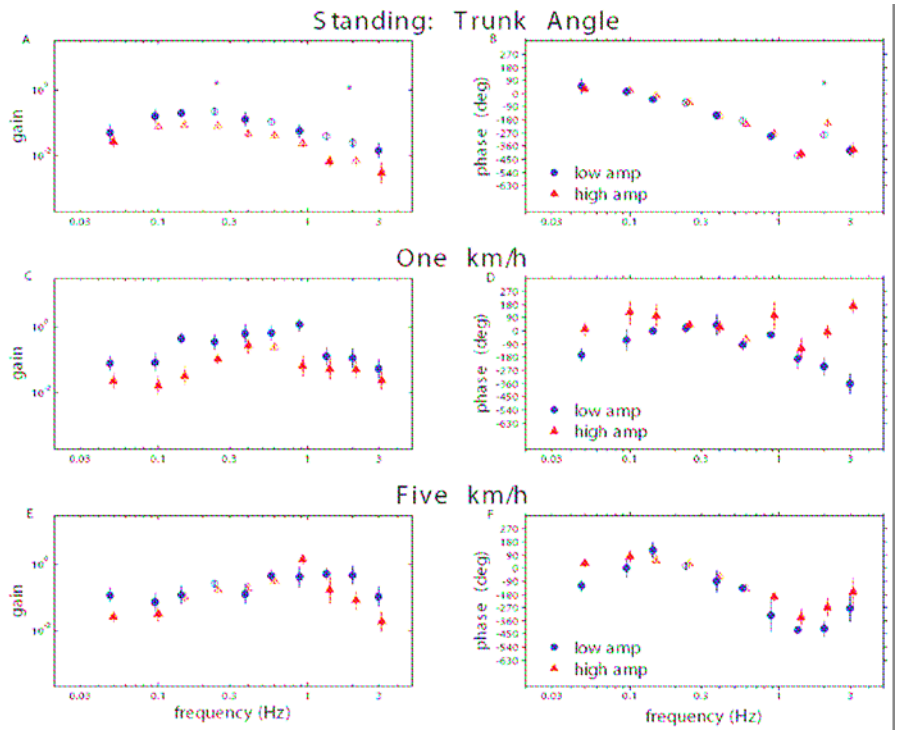

Figure 4.8. Gain and phase of trunk angle: amplitude effects. Gain and phase of trunk angle with visual scene motion in each condition. Open face symbols represent those frequency bins where gains were different from zero. Asterisks represent significant, real differences in amplitude (α=.05). Error bars are bootstrapped standard error (n=12).

In Figures 4.7-.8, it is clear that the only condition with consistent responses is the high amplitude posture condition. Figure 4.7A shows an amplitude dependent change in gain occurring in posture for the right leg angle in bin 3 while Figure 4.8A shows the same in the trunk at bin 4 and 10. These changes in gain make up 3 of the 10 amplitude dependent changes in gain observed in segment angles during standing posture in both sides of the body. The other amplitude dependent changes in gain occur in the left trunk (bins 3, 4 and 6), left leg (bin 2), left foot (bins 2 and 6), and right foot (bin 6). Seen in Figure 4.8A, the only amplitude comparison that was possible in a segment angle during locomotion was observed in bin 4 at 5 km/ in the

trunk angle. In this specific case, an amplitude dependent change in gain was not observed.

As there are no instances where both leg and trunk responses to visual scene motion are real at the same bin during locomotion conditions, it is impossible to compare gains of leg and trunk segments. This complication does not allow interactions of amplitude and segment to be tested in this investigation.

FRFs at the stride frequency

Figure 4.9 shows mean FRFs at the stride frequency with 95% confidence intervals in each condition for the ankle, knee, hip and shoulder on the right side of

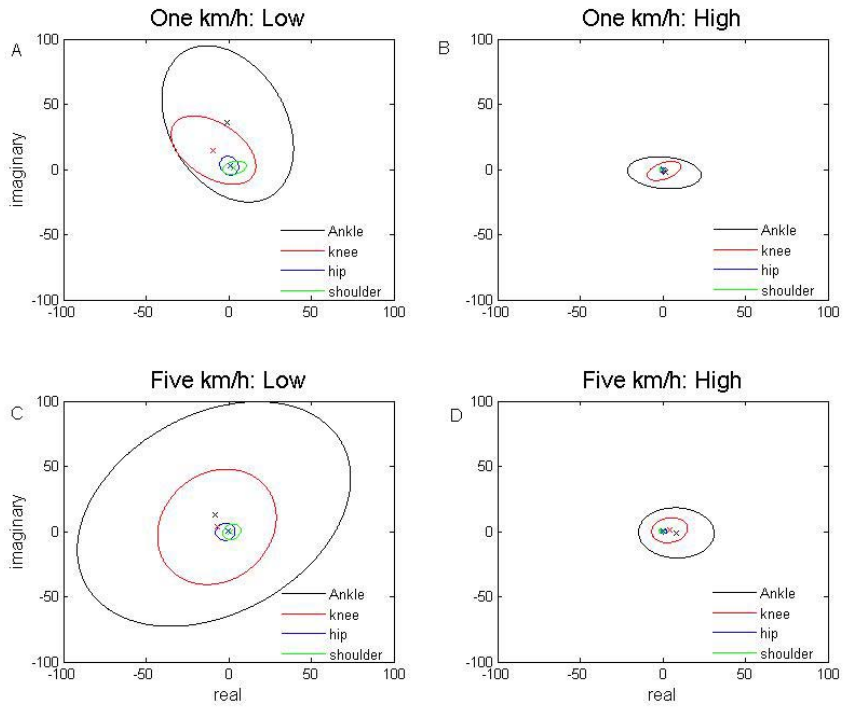

Figure 4.9. FRF at gait frequency. Means (x's) and 95% confidence ellipses of FRFs of right A/P displacements of ankle, knee, hip, and shoulder to visual scene motion. PSDs and CSDs are normalized to the gait cycle frequency in each trial prior to averaging across trials to compute these FRFs (n=12).

the body. Across locomotion conditions, these ellipses are larger in the ankle than the knee and larger in the knee than the hip and shoulder. There is not a clear distinction

in the size of the ellipses between hip and shoulder. These ellipses of the transfer functions are quite large because gains are large while phases are highly variable. Mean gain in the one km/h: low amplitude condition was 35.92 for the ankle and 2.78 for the shoulder. Additionally, mean gain in the one km/h: high condition was 2.80 for the ankle and .81 for the shoulder. Mean gain for the ankle was 15.08 while the shoulder's mean gain was 1.01 in the five km/h: low condition. Finally, mean gain in the five km/h: high condition was 8.08 for the ankle and .66 for the shoulder. Yet, there is not a distinct phase relationship because all of these confidence intervals of the FRFs contain 0. As a result of these erratic phases, initial tests of significance show that all kinematics do not show real responses to the visual scene at the frequency of gait (α=.05).

Chapter 5: "Visual Influence on Trunk Stability during Locomotion"

Motivated by the findings in chapter 4, a manuscript was prepared that investigates the differing responses of the trunk's displacements and segment angle to changes in visual scene motion. This manuscript also investigates dependence of these responses on phase of gait cycle, general biomechanics measures of gait and gross measures of variance that may explain the "freezing" illusion.

Visual Influence on Trunk Stability During Locomotion

David Logan[1], Tim Kiemel[1], Nadia Dominici[2], Germana Cappellini[2], Yuri Ivanenko[2], Francesco Lacquaniti[2,3], John J. Jeka[1,4,5]

Department of Kinesiology[1],
Neuroscience and Cognitive Science Program[4],
Biomedical Engineering Graduate Program[5],
University of Maryland
College Park, MD 20742

Laboratory of Human Neurophysiology[2]
IRCCS Santa Lucia Foundation
University of Rome Tor Vergata[3]
Rome, Italy

Corresponding author:
John J. Jeka
Department of Kinesiology
2357 SPH Building
University of Maryland
College Park, MD 20742-2611
Tel: 301 – 405 – 2512
Fax: 301 – 405 – 5578
Email: jjeka@umd.edu

Keywords: Locomotion – Postural Stability - Vision - Optic Flow

Acknowledgments:Support for this research provided by: NIH grant NS35070 (John Jeka, PI) and the Santa Lucia Foundation (F. Lacquaniti)

The evolutionary development of bipedal stance, which freed the hands from locomotion, is considered the fundamental distinction between humans and our closest relatives. Accompanying that development is the problem of stability. Engineered devices, such as cars and robots, typically solve the stability problem by having a wide base of support and/or concentrating the bulk of its weight lower down. However, the human body has evolved with more than just upright stability as a constraint, with most of its mass concentrated higher up in the trunk, making it inherently unstable and prone to falls. Here we investigate the problem of bipedal upright stability on both a fixed and moving base of support.

During locomotion, vision takes on an expanded role when compared to standing posture, supporting behaviors such as navigation and obstacle avoidance (e.g., Patla, 1997; Schubert et al., 2003; Warren, 2004). Studies have shown that optic flow has a modulating effect on gait speed (Konczak, 1994; Lamontagne et al., 2007) as well as properties of the gait cycle, such as stride length (Prokop et al., 1997). Such studies, however, offer little in terms of the role of vision for self-motion estimation and the online corrections for upright stability during locomotion. Here we use broadband visual stimuli, not optic flow, to illustrate how vision plays the dual role of correcting ongoing deviations from upright posture during locomotion (i.e., stability) as well as navigation.

Warren and colleagues were the first to consider using vision to probe postural stability during locomotion (Warren et al, 1996; Kay & Warren, 2001)). Using sinusoidal visual stimulation at selective frequencies much lower than those associated with the gait cycle (i.e., 0.25 Hz), definitive body sway responses to the

low-frequency visual stimuli were observed, which were linked to properties of the optic array (i.e., motion parallax). However, probing postural stability during locomotion with periodic sensory stimuli is not as straightforward as during standing. Postural control is often characterized as a linear stochastic system, essentially a fixed point attractor with noise, allowing application of linear systems methods such as spectral analysis (e.g., gain and phase) to capture frequency dependent relationships between body sway and sensory inputs during upright standing (Peterka, 2002; (Kiemel, Oie, & Jeka, 2006). Locomotion entails limit-cycle dynamics due to the periodic nature of the gait cycle, introducing nonlinearities that limit direct application of linear systems techniques. For example, spectral analysis of locomotion demonstrates a peak not only at the frequency of the gait cycle but at successive harmonics, a clear signature of a nonlinear process. The spillover of power into neighboring frequencies makes it difficult to interpret a response to a visual stimulus as due to the stimulus alone. Due to these concerns, we focus our analysis of how vision influences locomotion into the trunk, as we provide evidence below that the trunk is not dependent upon different phases of the gait cycle, justifying a linear approach to its analysis. Our focus on the trunk stems as well from its critical importance to the control problem as the most massive body segment (Mackinnon & Winter, 1993)

A second critical difference between posture and locomotion is the obvious change in the control problem from a fixed to a moving base of support. Upright bipedal postural control is thought to consist of two essential processes: to maintain equilibrium in response to perturbations and to maintain orientation to vertical (Horak

& Macpherson, 1996). These two processes are inherently linked during standing, as angular deviations of the body lead to both a change in translation and a change in orientation. However, when freed from a fixed base of support during locomotion, this proportional relationship between translation and orientation no longer holds. We argue that a moving base of support leads to a fundamental separation of how vision influences different processes related to the control of upright stability during locomotion.

Methods

Subjects

Twelve healthy subjects [5 males and 7 females, between 20 and 31 yrs of age, 69.4 ± 16.2 kg] received financial compensation for participating in this study. All subjects were self reported to have no history of balance disorders or dementia, and were not using prescription drugs that affect balance. Additionally, subjects had no history of surgical procedures involving the feet, ankles, knees, hips, back, brain, spinal cord or inner ear. The studies conformed to the Declaration of Helsinki, and informed consent was obtained from all participants according to the procedures of the Ethics Committee of the Santa Lucia Institute.

Apparatus

Virtual reality environment. Subjects walked or stood on a treadmill (EN-TRED 1475.911, Enraf-Nonius, Netherlands) one meter in front of a translucent screen (4x4m) with a rear-projected virtual display with dimensions 2.55 m wide by 1.82 m high at position 0**,** as shown in Figure 4.1**.** Subjects wore goggles with occluded sides to prevent them from seeing the border of the visual display, which

consisted of 500 randomly-distributed white triangles (2.6 x 2.6 x 2.4 cm) on a black background, updated at 60 Hz. The virtual display was created using CaveLib software (Mechdyne, USA) with projection through a digital projector (MP3135, HP,USA) synched to a desktop computer (Precision PWS490, Dell, USA). Visual signals were created offline (Matlab, Mathworks, USA) and generated via Labview (National Instruments, USA) on a desktop computer (Pentium 4, HP, USA).

Visual scene signals. These driving visual signals were either a high or low amplitude filtered white noise signal that translated in the sagittal plane. For each trial of each subject, a different seed was used to generate a white noise signal using a random number generator. High amplitude signals had a one-sided spectral density of 156.8 cm^2/Hz while low amplitude signals had a spectral density of 9.8 cm^2/Hz, as shown in Figure 4.2. These signals were then filtered using a first-order Butterworth low-pass filter with a cutoff of .02 Hz and an eighth-order Butterworth low-pass filter of 5 Hz. In doing so, power of scene motion was concentrated in lower frequencies where postural responses to sensory inputs are known to occur. Across subjects and speeds, the high amplitude signal had an average RMSE of ± 1.989 cm and ± 3.499 cm/s while the low amplitude signal had an average RMSE of ± .523 cm and ± .878 cm/s. A positive/negative signal corresponded to an anterior/posterior translation. A one cm negative translation of the visual scene corresponded to an expansion of the triangles to 3.4 x 3.4 x 3.2 cm. Visual display generation and data collection software were synchronized via an external trigger.

Kinematics. Body kinematics were measured using a VICON motion capture system (VICON,Inc, Oxford, UK). Reflective markers were placed on the right and

left sides of the body at each of the following landmarks: the base of the 5th metatarsal, the posterior calcaneus (heel), the lateral malleolus (ankle), the lateral femoral condyle (knee), the greater trochanter (hip), and the acromion process (shoulder). All kinematic data were collected at 100 Hz.

To investigate the influence of visual signals on the trunk, our analysis focuses on shoulder and hip markers averaged across both sides of the body in addition to their difference. The difference between shoulder and hip translation in the sagittal plane is a small angle approximation of the trunk angle and allows us to directly compare this measure of trunk orientation with measures of trunk translation (i.e., same units). Leg kinematics were used to calculate gait cycle measures and phase-dependent cross-covariance functions to justify a linear systems analysis (see *phase-dependent cross-covariance* below).

Procedures

Prior to experimentation, subjects experienced a static visual display at the experimental locomotion speeds. Subjects began each experimental trial by looking straight ahead at the visual display screen. Once they were ready, subjects said "Go" and the experimenter initiated treadmill movement for approximately 30 seconds for the subject to reach steady-state. At this point, the subject would declare if he or she was ready for the trial to begin. The experimenter then initiated data acquisition/scene translation with variable delays to avoid start-up effects. Each trial was 120 seconds in duration with a rest of 60 seconds in between trials. The experimental design consisted of two amplitudes of visual scene motion (low-high) and three treadmill speeds (0, 1, 5 km/hr) for a total of six conditions.

Analysis

General biomechanics measures and motion variance. Using kinematics of the right leg, general gait measures and their coefficients of variation were calculated during locomotion conditions. Each heel-strike was computed as the local minima of heel marker in vertical plane while each toe-off event was identified from limb axis minima. The limb axis minima were defined as the local minima of the angle formed by the fifth metatarsal-hip axis in the sagittal plane. Gait period for each trial was the average length of time between toe-off events. Time in stance for each trial was the average time between heel strike and toe-off. Stride length was computed as the average A/P movement of the heel marker between successive heel strikes.

In addition to gait cycle variability, measures of gross variability of the A/P translation of shoulder, hip and approximate trunk angle were computed. For position and velocity variance, integrals of their power spectral densities were computed after averaging across trials within condition. Across-subject geometric means of these variances are plotted with ± standard error.

Phase-dependent cross-covariance. Normalized phase-dependent cross-covariance functions between the velocity of the visual scene $s(t)$ and a kinematic variable $x(t)$ were defined as

$$c(\tau;\theta^*) = \mathrm{Cov}[s(t-\tau), x(t) | \theta(t) = \theta^*] / \sigma_s ,$$

where τ is time lag and θ^* is a value of absolute phase. Absolute phase $\theta(t)$ was defined using the heel-strike times t_1, t_2, ... for a given reference leg. Specifically, if $t_i \leq t < t_{i+1}$, then $\theta(t)=(t - t_i)/(t_{i+1} - t_i)$. The cross-covariance is normalized by dividing by the standard deviation σ_s of $s(t)$ so that $c(\tau;\theta^*)$ has the same units as $x(t)$. We

computed separate cross-covariance functions using the left and right legs as the reference and then we took the average of both functions.

Frequency response functions: gain and phase. Measures of gain and phase were computed from the frequency response functions (FRFs) of the A/P translation of shoulder, hip and approximate trunk angle to visual scene motion. First, Fourier transforms of the de-meaned visual scene translations (*x(t)*) and these de-meaned kinematics (*y(t)*) were calculated. One-sided power spectral densities (PSDs) and cross spectral densities (CSDs) using Welch's method with a 20 second Hanning window and one-half overlap were then calculated with these transforms. These PSDs and CSDs were then averaged within condition for each subject. For each subject, PSDs and CSDs of stimulus frequencies up to 3.7 Hz were binned linearly on a logarithmic scale to create ten frequency bins. Stimulus frequencies in the following ranges created the ten bins: .05, .1, .15, .2-.3, .35-.45, .5-.7, .75-1.1, 1.15-1.65, 1.7-2.5, and 2.55-3.7 Hz. For plotting purposes, binning these stimulus frequencies yielded bin averages of .05, .1, .15, .25, .4, .6, .925, 1.4, 2.1 and 3.125 Hz.

Using these binned PSDs and CSDs, complex coherence was calculated as $\boldsymbol{c_{xy}(f) = P_{xy}(f)/\sqrt{P_{xx}(f)P_{yy}(f)}}$. Across subjects, the FRF was defined as $\boldsymbol{\bar{H}_{xy}(f) = \bar{c}_{xy}(f)\sqrt{\bar{P}_{yy}(f)/\bar{P}_{xx}(f)}}$ where $\boldsymbol{\bar{c}_{xy}(f)}$ is the mean complex coherence and $\boldsymbol{\bar{P}_{yy}(f)}$ and $\boldsymbol{\bar{P}_{xx}(f)}$ are geometric mean PSDs (Kiemel, Elahi, & Jeka, 2008).Although this method weights subjects with higher coherences in each bin, we believe this method is suitable as it is common place in similar studies (Warren et al, 1996, Kay and Warren, 2001) to analyze those results found from responders when subjects are

initially divided into those whose movements are affected by visual scene motion and those who are not.

The outcome measures used to characterize these FRFs were gain and phase. Gain is the absolute value of $\bar{H}_{xy}(f)$ and phase is the argument of $\bar{H}_{xy}(f)$, converted to degrees. A gain of one indicates a proportional response of $y(t)$ to $x(t)$ while a positive phase indicates that $y(t)$ was phase advanced relative to $x(t)$.

Statistics

To test whether the cross-covariance function depended on absolute phase for some bin $(\tau_1, \tau_2]$ of time lags, we averaged $c(\tau;\theta^*)$ over the time lags in the bin to obtain $\bar{c}(\theta^*)$. We then approximated $\bar{c}(\theta^*)$ by a Fourier series with a constant term and four modes:

$$\bar{c}(\theta^*) \approx a_0 + \sum_{m=1}^{4}\left[a_m \cos(2\pi\theta^*) + b_m \sin(2\pi\theta^*)\right].$$

Using values of the coefficients for each subject, we applied a t-test to a_0 to test whether the constant term was nonzero and we applied Hotelling's T^2 to the vector (a_m, b_m) to test whether each mode was nonzero. We used a significance level of 0.05 with a Bonferroni factor of 5 to adjust for the number of tests.

Due to our probe of a relatively wide band of frequencies, the first statistical tests for FRFs were determining if lower bounds on gain in each bin of each condition were greater than zero. First, 95% confidence intervals for log gain and phase of these FRFs were computed using the bootstrap percentile-*t* method with 4000 bootstrap resamplings and 400 nested bootstrap resamplings for variance estimation (Zoubir and Boashash, 1998). These FRFs were considered real, with gain greater than zero,

when this confidence region was different from 0 in the complex plane (α=.05).Log gain and phase are plotted with error bars representing ± standard deviation of 10,000 bootstrapped resamplings using the percentile t-method (Zoubir and Boashash, 1998).

To compare log gain and phase between amplitude, speed, and kinematic output; 95% bootstrap confidence intervals were computed for differences in log gain and differences in phase. Interaction effects were identified by computing differences of these log gain differences and phase differences. Differences in gain and phase were found when these confidence intervals did not include one and zero, respectively. Changes in log gain and phase are illustrated by plotting mean gain ratios and phase differences with their 95% confidence intervals.

Two-way (2 speeds x 2 amplitudes) repeated measures ANOVAs with Greenhouse-Geisser adjustment were used each general biomechanics measures and their coefficients of variation (α=.05). For measures of position and velocity variance, three-way (3 speeds x 2 amplitudes x 3 kinematic outputs) repeated measures ANOVAs with Greenhouse-Geisser adjustment were performed on geometric means of position and velocity variance (α=.05).

Results

Phase dependence: Trunk-Leg Segments

In general, the effect of visual scene motion on a kinematic variable depends on when during the gait cycle the kinematic variable is measured. To investigate such phase-dependent effects, we computed normalized phase-dependent cross-covariance functions $c(\tau;\theta^*)$ between the velocity of the visual scene and a kinematic

variable $x(t)$. Heel strikes of a reference leg were used to define absolute phase for the gait cycle.

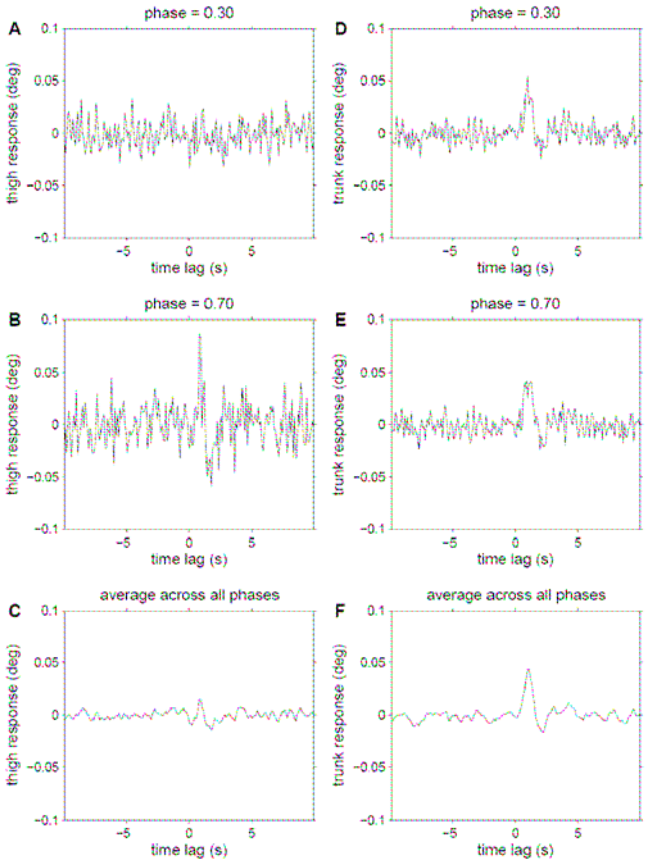

Figure 5.1. Cross-covariance. Phase dependent cross-covariance functions for the (a-c) trunk angle and (d-f) thigh angle.

Figure 5.1 illustrates the phase-dependent analysis for 5km/h walking with large amplitude visual-scene motion. Figure 5.1A-B shows $c(\tau;\theta^*)$ for the thigh angle on the same side as the reference leg for values of absolute phase $\theta^* = 0.3$ and $\theta^* = 0.7$. Note that there is a clear peak in the cross-covariance function for small positive time lags for $\theta^* = 0.7$ (Fig. 5.1B), indicating that at this phase of the gait cycle the thigh angle is correlated with previous values of the velocity of the visual scene. However, at phase $\theta^* = 0.3$ a peak is no longer evident (Fig. 5.1A),

demonstrating that the effect of visual scene motion depends on the phase of gait of cycle. Averaging across all phases of the gait cycle (Fig. 5.1C), there is some suggestion of a peak in the cross covariance function, but it is much smaller than the peak at specific phases such as $\theta^* = 0.7$ (Fig. 5.1B).

The extent to which the effect of visual scene motion depends on phase was different for different kinematic variables. For example, the trunk angle showed less phase dependence than the thigh angle. The cross-covariance functions for the phases $\theta^* = 0.3$ and $\theta^* = 0.7$ (Fig. 5.1D-E) were not dramatically different than the mean cross-covariance function (Fig. 5.1F).

Figure 5.2 shows the phase dependence of the cross-covariance functions for the thigh and trunk angles over different ranges of time lags. For each angle, we show $c(\tau;\theta^*)$ averaged over a range of time lags that includes the peaks seen in Fig. 5.1 (solid lines) and a range of larger time lags (dashed lines). For the thigh angle (Fig. 5.2A), $c(\tau;\theta^*)$ from 0.5 to 1.0 s showed significant phase dependence (Bonferroni adjusted $p < 0.005$). Note that the cross-covariance is largest near phase 0.7 of the gait cycle, which corresponds to the clear peak in Fig. 5.1B. For time lags from 1.5 to 2.0 s, the phase-dependence is not significant.

For the trunk angle (Fig. 5.2B), $c(\tau;\theta^*)$ is not phase-dependent in both of the time-lag ranges shown ($p > 0.05$). However, the average of $c(\tau;\theta^*)$ across θ^* is significantly positive for time lags from 1.0 to 1.5 s and is significantly negative for time lags from 2.0 to 2.5 s ($p < 0.001$). For other ranges of time lags not shown in Fig. 5.2B, the cross-covariance does show some phase-dependence, but Fig. 5.2B

illustrates that the cross-covariance as a function of time lag is *qualitatively* similar for all phases of the gait cycle: a positive peak followed by a negative undershoot.

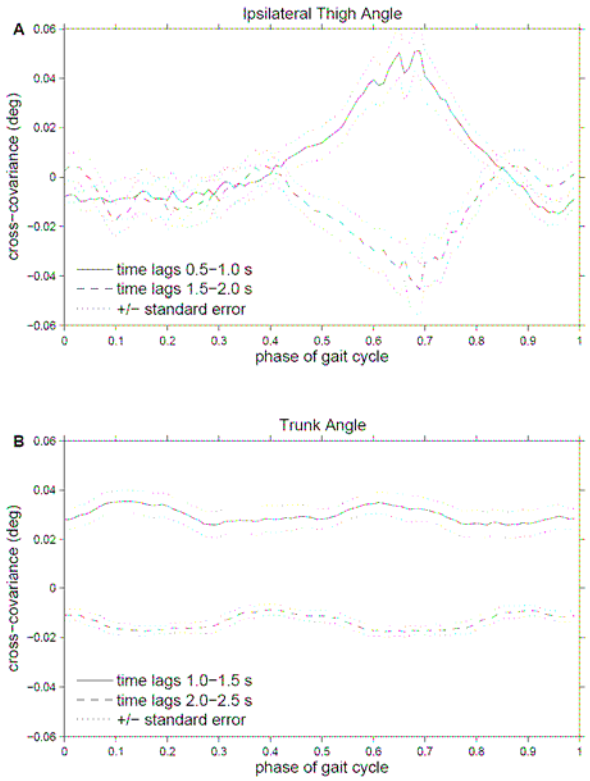

Figure 5.2. Phase Dependent Cross-covariance. Cross-covariance in 5 km/h: High condition in the(A) thigh and (B) trunk.

Due to the marked phase-dependence of the leg segment in response to the visual stimulus, we focus our analysis below on the relationship of the trunk to the visual stimulus. Analysis of the leg segment using nonlinear methods will be the focus of a subsequent paper.

Gain-phase

Initial tests of significance revealed that in the low amplitude conditions, gain of the trunk was different from zero in a small number of frequency bins (standing- 8/30; 1 km/hr - 2/30; 5 km/hr – 3/30, α=.05). Representative of these trends, the

responses of the shoulder in Figure 5.3 show that real responses of the body to the visual scene are much more evident in the high amplitude conditions and are concentrated in the low to middle frequency range. Due to the inconsistent responses in low amplitude conditions, we focus on high amplitude visual scene motion and its effects on translation and orientation of the trunk.

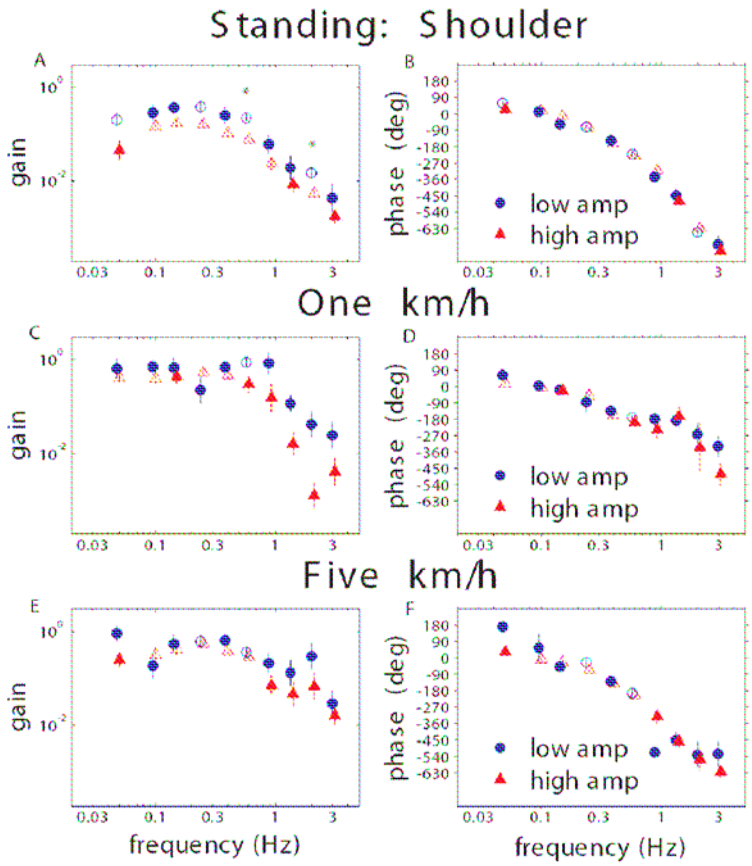

Figure 5.3. Gain and phase: amplitude effects. Gain and phase of A/P shoulder displacement with visual scene motion in each condition. Open face symbols represent those frequency bins where gains were different from zero. Asterisks represent significant, real differences in amplitude (α=.05). Error bars are bootstrapped standard error.

Figure 5.4A shows that gains of the hip and trunk angle in standing posture are not different from each other at the frequency bins where all trunk kinematics are different from zero. Gains of the shoulder are higher than both the hip and trunk angle

at all of these bins. In Figure 5.4B, the phase of all trunk kinematics showed the expected lead of the visual stimulus at low frequencies and a lag of the visual stimulus above the .15 Hz bin. No phase differences were observed for trunk kinematics during standing posture, except at the .25 Hz bin, in which trunk angle phase was slightly higher than the hip and shoulder.

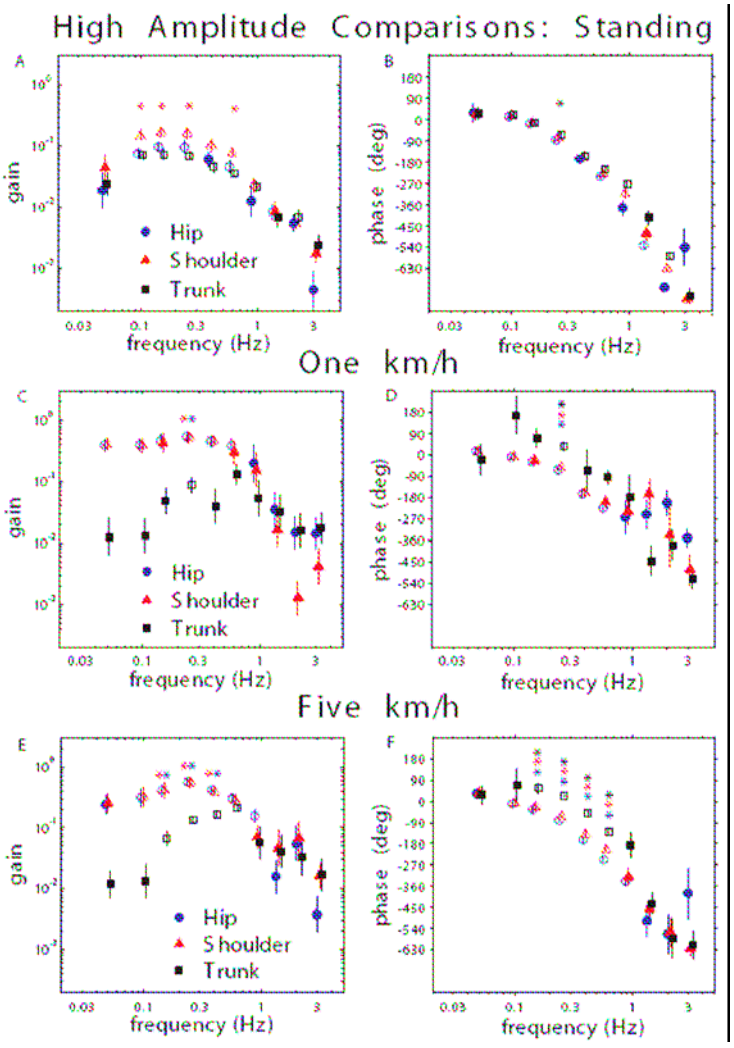

Figure 5.4. Gain and phase: translation versus orientation. Gain and phase of A/P translation of hip, shoulder and approximate trunk angle with visual scene motion at each speed. Open face symbols represent those frequency bins where gains were different from zero. Asterisks represent significant, real differences in kinematic output (α=.05). Single asterisks: kinematic output was higher than others with others not different from each other. Horizontal asterisks: two are greater than the other without being different from each other. Vertical asterisks: pair-wise comparisons reveal ranking order of all three. Error bars are bootstrapped standard error.

Clear differences in gain and phase in Figures 5.4C-D are evident among trunk kinematics between the posture and locomotion conditions. Compared to posture, there are significantly higher gains relative to vision for hip displacements in bins 2-4 and shoulder displacements in bins 4-5 in the 1 km/h condition. Trunk angle gain was different from zero only in frequency bin 4 (.25 Hz) and does not increase from posture to one km/h. Phase increases significantly at bin 4 for both the trunk angle and the shoulder.

When comparing the 5 km/h walking condition to posture, there are significantly higher gains to vision at 5 km/h for hip displacements in bins 2-4 and 6. In bins 4-6, gains of shoulder displacements at five km/h are significantly higher than posture. Additionally, trunk angle gain in bin 4 was significantly higher at 5 km/h than standing posture. Gain of the approximate trunk angle to vision at this bin was also significantly higher in 5 km/h than 1 km/h. There were no detectable differences in gain or phase when comparing the 1km/h and 5 km/h conditions for both shoulder and hip.

During locomotion, comparisons of gain and phase among trunk kinematics reveal a separation in measures of translation (hip and shoulder) and orientation (trunk angle). In bin 4 (.25 Hz) of Figure 5.4C, gain of both hip and shoulder displacement to vision are significantly higher than approximate trunk angle without being different from each other. There is also a phase difference of all trunk kinematics in this bin, as seen in Figure 5.4D.

As more consistent responses of the trunk angle are found in the 5 km/h condition, differences among kinematics are observed at a broader range of

frequencies than at one km/h. Figure 5.4E shows shoulder and hip gains were significantly higher than approximate trunk angle gain in bins 3-5 without being different from each other. In Figure 5.4F, phase reveals a clear ranking order among kinematics in the 5 km/h condition in bins 3-6.

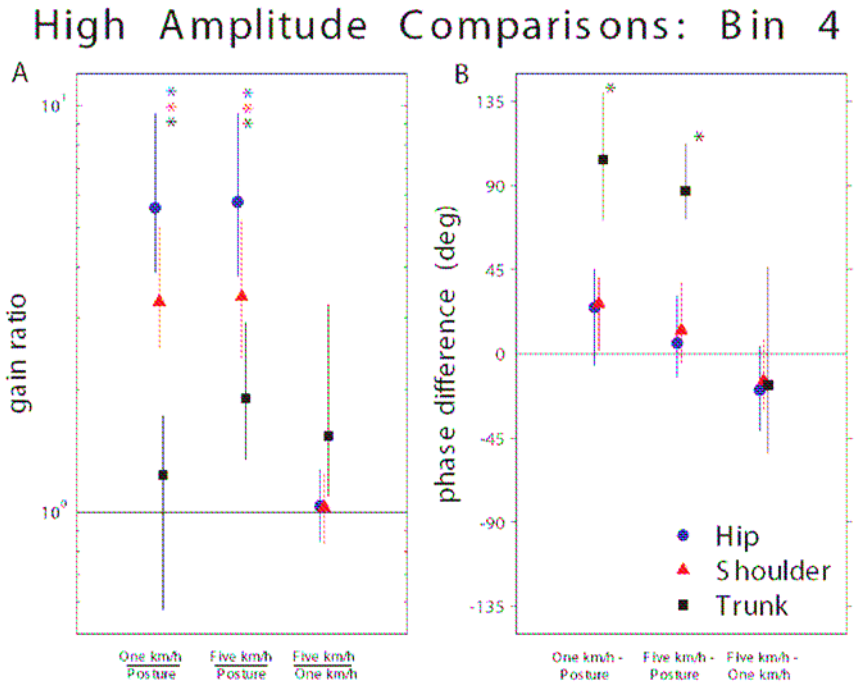

Figure 5.5. Interaction of speed and trunk kinematics. Gain ratios and phase differences of each trunk kinematic in bin 4 (.2, .25 and .3 Hz) for all possible speed comparisons in high amplitude conditions. Error bars are bootstrapped 95% confidence intervals (CIs); significant effects of speed occur when CIs of these gain ratios cross one or phase differences cross 0^0. Significant interaction effects are noted with asterisks. Single asterisks: Increase in phase due to changes in speed are greater in a single kinematic than other two kinematics without their respective changes being different from each other. Vertical asterisks: pair-wise comparisons of gain ratios reveal ranking order of all three gain ratios.

Figure 5.5 illustrates this interaction of kinematic and speed in the bin (4) where all trunk kinematics had a definite response to visual scene motion at all speeds. In Figure 5.5A, significant differences in gain ratios are observed between the trunk kinematics in comparisons of locomotion to posture. Comparing one km/h to posture, mean gain ratio of the hip was 5.59 and higher than the mean gain ratio of the shoulder at 3.29. Both gain ratios of hip and shoulder translation were higher than

the ratio found in trunk angle, whose gain ratio was not different from one. Comparing five km/h to posture, mean gain ratio of the hip was 5.79 and higher than the shoulder's of 3.38, which were both higher than the trunk angle's gain ratio of 1.9. Although the trunk angle had a significant gain ratio of 1.54, there were no differences in gain ratios across kinematics when comparing five km/h to one km/h.

Higher phase differences of the trunk angle in comparison to the hip and shoulder are seen in Figure 5.5B. Comparing one km/h to standing posture, the mean phase difference of 104º in the trunk angle is much higher than 27º found in the shoulder. Shoulder phase difference was not significantly different than the hip, whose phase did not increase. Comparing five km/h to posture, the mean phase difference of 87º in the trunk angle was higher than non-significant phase differences of shoulder and hip. No increases in phase or differences among kinematics were observed between locomotion conditions in this bin.

Kinematic variance and scene stabilization

With all kinematic variables, position variance was higher in both locomotion conditions compared to the posture condition, with no differences between 1km/h and 5 km/h. Significant interactions of kinematics and speed ($F_{2, 22}$=36.87, p<.0001), amplitude and speed ($F_{2, 22}$=4.89, p=.0223), and amplitude and kinematics ($F_{2, 22}$=6.43, p=.0162) were found for position variance. In the posture condition, Figure 5.6A shows higher shoulder position variance than the hip and trunk angle and no difference between the hip and trunk angle. An increase in position variance due to increased visual amplitude was observed at the shoulder only in the posture condition.

In both locomotive conditions, displacements of shoulder and hip had higher position variance than trunk angle.

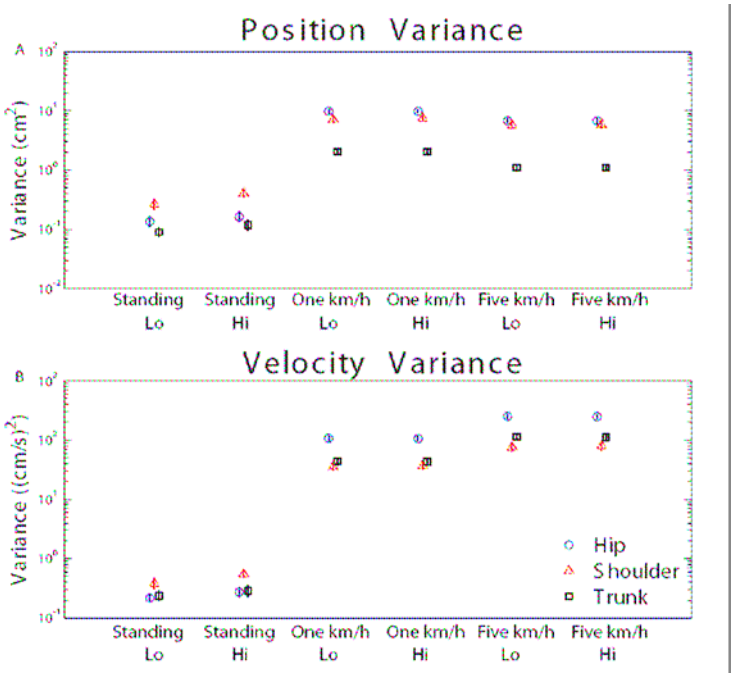

Figure 5.6. Variance: position and velocity. A: Geometric means of position variance. B: Geometric means of velocity variance. Error bars are standard error of the mean.

Interactions of kinematics and speed ($F_{2, 22}$=22.34, p<.0001), amplitude and speed ($F_{2, 22}$=8.25, p=.0103), and amplitude and kinematics ($F_{2, 22}$=6.49, p=.0109) were also found for velocity variance. As seen in Figure 5.6B, there were no differences in velocity variance between the hip and trunk angle during posture conditions. Shoulder variance increased with visual amplitude only during the posture condition. In the posture condition, velocity variance of the shoulder was higher than both the hip and trunk angle, regardless of visual amplitude. In both locomotive conditions, hip displacement had higher velocity variance than both shoulder displacement and trunk angle. In all kinematics, increases in velocity variance from posture to 1 km/h and 1 km/h to 5 km/h were found.

Freezing Illusion. In the standing posture condition, all subjects perceived movement of the visual scene. This movement is ambiguous, meaning that subjects cannot differentiate different conditions (e.g., visual amplitude). In contrast, all subjects reported that the moving visual scene stabilized during 1km/h and 5 km/h conditions, in other words, it looked like a solid wall of triangles with no movement. Essentially, subjects reported the screen as "frozen" during locomotion conditions. We discuss possible explanations of this illusion below.

General biomechanics measures. Table 5.1 shows how all general measures of gait biomechanics and respective coefficients of variation (C_v) were significantly affected by treadmill speed without an interaction of amplitude (α=.05). Increasing treadmill speed from one km/h to five km/h caused decreased gait period, decreased stance time, decreased percentage of gait cycle spent in stance, and increased stride length. Additionally, coefficients of variation for all measures decreased as speed increased ($p<.0001$ for all speed main effects).

General Gait Measures

Measure	1 km/h, low amp	1 km/h, high amp	5 km/h, low amp	5 km/h, high amp
Gait Period* (Sec)	2.38	2.39	1.04	1.04
C_V*	0.06	0.05	0.01	0.01
Stance Duration* (Sec)	1.78	1.78	0.66	0.66
C_V*	0.07	0.06	0.02	0.02
% Stance* (Gait Cycle)	74.61	74.44	63.08	63.10
C_V*	0.03	0.03	0.01	0.01
Stride Length* (cm)	102.14	102.50	154.83	154.68
C_V*	0.06	0.06	0.01	0.01

Table 5.1. General biomechanical measures of gait. C_v is coefficient of variation for corresponding gait measure. *denotes significance of speed main effect ($p<.0001$).

Discussion

Investigations of how the nervous system processes vision for locomotion typically use optic flow, in which the visual array moves coherently to simulate visual motion during over ground locomotion, to investigate how vision influences the characteristics of the gait cycle (e.g., Prokop et al., 1997). Here we implemented a different approach, presenting broadband visual stimulation that oscillated in the anterior-posterior direction. The intent was two-fold: 1) to understand how vision affects fluctuations of the body as it moves and maintains upright stance; and 2) to compare the influence of vision during standing posture and locomotion. Our findings support the idea that, unlike during standing posture, vision plays a dual role during locomotion, serving both upright stability and navigation.

Gain & Phase: Posture vs. Locomotion

One of the most striking findings was the large increase in gain for the hip and shoulder from the posture to the locomotion conditions, illustrated by the gain ratios in Figure 5.5. Gain ratios comparing posture and locomotion conditions ranged from 3-5, reflecting large gain changes, while those comparing locomotion conditions were close to one, reflecting only minor differences in gain. At the same time, gain ratios for the trunk angle were close to one and changed little across different comparisons, indicating consistent gain values for the posture and locomotion conditions. The distinct behavior of the individual joints compared to the trunk segment is further emphasized in Figure 5.4, showing gain values in each condition. While gain is similar for all kinematic variables in the posture condition, hip and shoulder gain

increase dramatically during both locomotion conditions while trunk angle gain remains at the level observed with posture.

These differences in gain change between joint translation and trunk orientation derive from the fact that the base of support is no longer fixed during locomotion, allowing the body to translate freely in the anterior-posterior direction, at least within the constraints of the treadmill surface. From this perspective, the increased gain to the visual motion during locomotion may reflect a change in the control strategy between posture and locomotion, making the anterior-posterior direction less resistant to perturbation (i.e., less stable) and freeing the body to navigate through the environment in response to visual stimulation. The result is large trunk displacements relative to visual motion when compared to trunk orientation, which remains resistant to visual perturbation during both standing and locomotion. Thus, increases in hip and shoulder gain reflect decreased stability to enhance navigation rather than an increase in coupling to enhance upright stability.

Drastically different between posture and locomotion, increases in phase observed in the trunk reflect the anchoring of the trunk segment. As seen in Figure 6, the phase of the trunk increases in a systematic fashion in the middle range of frequencies during locomotion while only small changes in phase are observed in joint translations, if at all. In standing posture, probing postural sway at a broad range of frequencies reveals that the trunk motion will lead the visual scene motion until some fundamental frequency of postural sway and then lags the visual stimulus thereafter at higher frequencies (Peterka, 2002; Kiemel et al, 2006. These increases in phase mean that the trunk segment is leading the visual display to a greater degree

and maintains this lead into a higher frequency range than typically seen in standing posture. Additionally, these trunk phases separate from joint translations and continue to lead them as they both lag the motion of the visual scene. These significant phase leads of the trunk are likely due to the trunk angle having a higher fundamental frequency during locomotion than standing posture. This causes the lower frequency lead-lag behavior to be shifted to higher frequencies, and crossing phase 0º to occur at a later frequency bin.

Overall, these results are consistent with evidence indicating that the anterior-posterior plane is less actively controlled than the medial-lateral direction during locomotion (Bauby & Kuo, 2000; Donelan, Shipman, Kram, & Kuo, 2004); Warren et al, 1996). Passive stability in the A/P plane (Kuo, 2007) may allow the nervous system to prioritize steering and navigation when controlling equilibrium. In fact it is arguable that stability, defined as the resistance to perturbations, is counter to the task of navigating through the environment, necessitating the need to diminish resistance to environmental changes.

Effect of Visual Amplitude

Numerous studies in human postural control have used linear systems techniques to establish how multisensory information is continually reweighted to maintain flexible and stable upright stance. One of the primary tools has been to change the amplitude of a sensory input such as vision and measure the corresponding sway response. Results have consistently shown an inverse relationship between gain and sensory amplitude (Kiemel et al., 2006; Peterka, 2002). For example, as visual amplitude increases (decreases), body sway gain decreases

(increases). The logic is that as visual amplitude increases, body sway cannot maintain the same level of coupling with vision without being driven towards its stability limits. Consequently, the visual channel is downweighted while other modalities are upweighted to maintain upright stability (Oie et al., 2002; Cenciarini & Peterka, 2006). Sensory reweighting is not modality specific but is a general principle of how sensory information is processed for standing posture.

Gain results in Figure 5.3 are consistent with the interpretation of sensory reweighting in the standing posture condition, but not with locomotion. There is a consistent decrease in gain with an increase in visual motion amplitude during standing posture, although statistical significance was found at only two frequency bins. Lack of significance across all frequencies may be partially due to the filtered white noise visual stimulus, which spreads the power of the stimulus across all frequencies and diminishes the response at any single frequency. Consequently, gain to the visual stimulus was less robust compared to previous studies of postural control which used sum-of-sines visual stimuli (Kiemel et al., 2006). Using a filtered white noise visual stimulus was motivated by the fact that significant peaks are observed in the power spectrum of body sway due to the limit cycle behavior of gait. If a visual stimulus frequency overlaps with gait cycle frequency (and its harmonics), it is difficult to distinguish the response to vision at that frequency. To compound matters, gait cycle frequencies differ across individuals, making it difficult to predefine at specific frequencies. Because filtered white noise contains power at all frequencies, it allows one to bin the frequencies so as to avoid such overlap.

Despite these technicalities, the interesting finding is the clear difference in the response to changes in visual amplitude between posture and locomotion. Body responses during locomotion showed none of the amplitude dependent effects that are well documented during standing posture. One possible explanation is that much larger amplitudes are required to observe visual reweighting during locomotion, as position and velocity variance are much larger during locomotion than posture (see Figure 5.6), making it difficult to detect small amplitude changes in the visual environment. Alternatively, because movement in the anterior-posterior direction is not constrained by a fixed base of support, reweighting due to a change in visual amplitude may not be functionally relevant, as an increase in visual amplitude can be matched for navigation. The lack of reweighting, however, may be direction dependent. The medial-lateral direction is far more constrained during locomotion and has been suggested to be under more active control than the anterior-posterior direction, which can take advantage of passive dynamics (Bauby & Kuo, 2000). A constrained support base may translate into properties more similar to posture and suggests that sensory reweighting is highly dependent on the characteristics of the support base.

Effects of Speed

We compared trunk behavior at two distinct speeds to understand how gait speed may alter the relationships we have observed. It is well known that increasing speed leads to a more linear relationship between step rate and stride length, among other biomechanical variables (Inman et al, 1980). Our results indicate that responses to visual stimulation also become more linear with speed, at least with the trunk. In

addition, while the thigh segment showed clear phase-dependent effects, the trunk behaved in a more linear manner, showing far less dependence on the gait cycle. The interaction of postural stability mechanisms and the rhythmic oscillations of the body due to the gait cycle clearly have some dependence on speed. These findings motivate further investigations into how visual information is used at different speeds of locomotion.

In sum, our use of a sensory probe to understand the comparison of posture and locomotion reveals the nervous system's priorities in controlling upright stability. As the behavior is changed from posture to locomotion, control of a translating equilibrium is no longer a priority for upright stability. The control problem of the massive trunk becomes maintaining orientation upright during destabilizing navigation with the ever-present threat of gravity.

Motion variance, scene stabilization and reweighting

In this investigation of upright stability, where responses (gain) of the body to a visual scene increased from posture to locomotion, a seemingly related perceptual effect occurred. All subjects reported that the visual display "froze" to become a solid wall during locomotion, unlike during standing posture when visual movement was evident. A similar perception of a slowing of visual movement has been noted in other contexts (Durgin et al., 2005; Pavard & Berthoz, 1977; Mesland & Wertheim, 1995). However, these studies have not attempted to characterize the visual display's influence on body movements to determine if this correlates with the perceptual effect.

Pavard and Berthoz (1977) accelerated subjects in a cart and instructed them to push a button when they perceived images in a head mounted display (HMD) to be stabilized. These authors suggested that this stabilization was a result of an underestimated image velocity due to an increased vestibular sensation over the actual image velocity. It has also been suggested that this effect is due to an efference copy created by multiple sensory inputs in order to stabilize the world as one moves their body (Probst et al., 1986).

Durgin and colleagues would later suggest an extension of Barlow's (1990) theory of sensory inhibition in a "multicue subtractive model" to explain reductions in perceived speed of optic flow. As the sum of reductions in perceived speed during passive motion and reductions in perceived speed during treadmill walking approximated that of over-ground walking in a HMD, these authors argued that perceived reductions in flow speed while walking are due to self-motion estimates by both motor and vestibular system (Durgin et al, 2005).

Wertheim and Reymond (2007) developed a mathematical model based upon a previous experiment where subjects estimated the relative velocity of a moving grating on a physically moving monitor (Mesland and Wertheim, 1995). Central to this model, a just noticeable difference (JND) term must be eclipsed by the sum of the velocity of a reference signal and velocity of the stimulus on the retina in order to perceive velocity of the stimulus. These authors' description of the JND includes neural noise while this reference signal is the sum of the efference copy and ego-motion (Wertheim & Reymond, 2007).

In our experiment, where subjects actually move with the translating display (see gains), translation sensations in addition to self generated estimates of motion affect the perception of a moving scene. Along the lines of Wertheim and Reymond, there is a JND at work and this term can be extended to the context of locomotion. Although increases in variability are expected in locomotion compared to standing, we've presented gross measures of position and velocity variance to justify our understanding of this freezing illusion. This increased self-motion during locomotion raises the JND of visual scene motion, requiring larger amplitudes for detection of the scene motion. A larger JND leads to the perception of a "frozen visual scene" when walking for the same visual amplitude that is perceived as moving during standing. Because the motor consequences of perception on a self-moving body are much different than one that is stationary with moving scene, there must be a distinction between those perceptions caused by a moving scene and those initiated by the moving body. Here, we make the distinction that an "ego-freeze" of visual scene motion occurs when the JND is raised a result of self-motion.

Unique to our study, this perceptual effect occurred regardless of the direction of image movement as the image was stabilized throughout the duration of the trial. In previous manipulations, the "Pavard & Berthoz effect" was strongest when images were moving in the opposite direction of one's motion. Our unpredictable filtered white noise signal created enough oscillation of the trunk and in turn the head that the neural noise created to accurately perceive image motion in either direction was exceedingly high. Yet, our higher gains during locomotion conditions reveal that the

nervous system was using this visual information in some way as the body was indeed moving with the visual scene.

As a result of this interaction with the motor control system, we hypothesize that this perceptual effect interferes with use of sensory reweighting during locomotion. During standing, gain decreases when amplitude of visual scene motion increases, reflecting downweighting of vision in a sensory stabilization process of sensory reweighting (Oie et al, 2002; Peterka et al, 2002). So far, it has been revealed that responses to visual scene motion do not occur in the same amplitude ranges of scene motion where responses in standing posture can be measured (Fig 5 A, C, E). Standing and locomotion may have different ranges of amplitudes over which reweighting is observed. Alternatively, reweighting is not necessary during locomotion because AP movement is less constrained during locomotion.

We suggest the latter to be correct; less constrained and more variable AP movement causes this "ego-freeze" which interferes with ongoing attempts of the nervous system to discriminate between stabilizing and destabilizing visual information. As a result, the body translates with the visual scene in a manner that threatens upright stability.

Chapter 6: Leg-Trunk Coordination

Here, the in-phase and out-of-phase behavior between the leg and the trunk observed in posture is investigated in locomotion. By calculating complex coherence, the strength and patterns of coordination in posture and locomotion are described to address hypothesis 4.

Methods

The same experimental data used in chapter four was used in this investigation. All methods and materials used are the same as chapter four except the data analysis.

Analysis

Complex Coherence. Complex coherence was computed from leg and trunk segment angles from vertical in the A/P plane using the ankle, hip and shoulder markers on the right side of the body. Means were first subtracted from these angles' trajectories. Next, one-sided power spectral densities (PSDs) and cross spectral densities (CSDs) using Welch's method with a 20 second Hanning window and one-half overlap were then calculated from these "de-meaned" angle trajectories. These PSDs and CSDs were then averaged within condition for each subject and had a frequency step of .05 Hz. Complex coherence was calculated as

$c_{xy}(f) = P_{xy}(f) / \sqrt{P_{xx}(f) P_{yy}(f)}$ where P_{xy} is the CSD between the leg and trunk and P_{xx} and P_{yy} are the PSDs of the leg and trunk, respectively. The magnitude of complex coherence is coherence (r) and the argument is the phase of complex coherence.

Normalized Complex Coherence. To compute normalized complex coherence, a multiple of the average gait period in each trial was used as the size of the spectral window for CSDs and PSDs for leg and trunk angle. Gait period for each trial was the average length of time between toe-off events, which were identified from leg axis minima. The leg axis minima were defined as the local minima of the angle formed by the fifth metatarsal-hip axis in the sagittal plane. Complex coherence was computed in the same manner as above with the only caveat being that the spectral window for each trial was ten multiplied by the average gait period for each trial.

Statistics

The primary interest of this analysis was to identify relationships between trunk and leg segments that were coherent during posture and locomotion. For complex coherence, significant relationships between trunk and leg were identified when the 95% confidence region of $c_{xy}(f)$ in the complex plane did not include zero (α=.05). Leg and trunk are considered in-phase when coherence is real and phase approximates 0º while leg and trunk are considered anti-phase when coherence is real and phase approximates either 180º or -180º.

Results

Figure 6.1 shows leg-trunk coherence (r) and phase of complex coherence in all conditions from 0 to 5 Hz. As seen in Figure 6.1 A-B, in-phase behavior of leg and trunk is observed in the low amplitude condition from .1 to .35 Hz and in the high amplitude condition from .1 to .5 Hz. Anti-phase behavior in standing posture is observed from 1.05 to 5 Hz in the low amplitude condition and from 1.1 to 5 Hz in the high amplitude condition. In the one km/h condition, as Figure 6.1 C-D shows,

the leg and trunk show in-phase behavior in the low amplitude condition from .35 to .6 Hz and in the high amplitude condition from .4 to .6 Hz. In one km/h, anti-phase behavior is observed from .8 to 5 Hz in both low and high amplitude conditions. At one km/h, however, mean phase in this region is 160º in the low amplitude and 164º in the high amplitude condition as there are noticeable dips in phase in this region. Figure 6.1 E-F shows in-phase behavior from .9 to 1.4 Hz in both the low and high amplitude condition of 5 km/h. Anti-phase behavior is observable from 1.8 to 3.3 Hz in the low amplitude condition and from 1.75 to 3.3 Hz in the high amplitude condition. At 3.85 Hz, however, there is a return of this anti-phase behavior in both low and high amplitude conditions for the remaining frequencies on display.

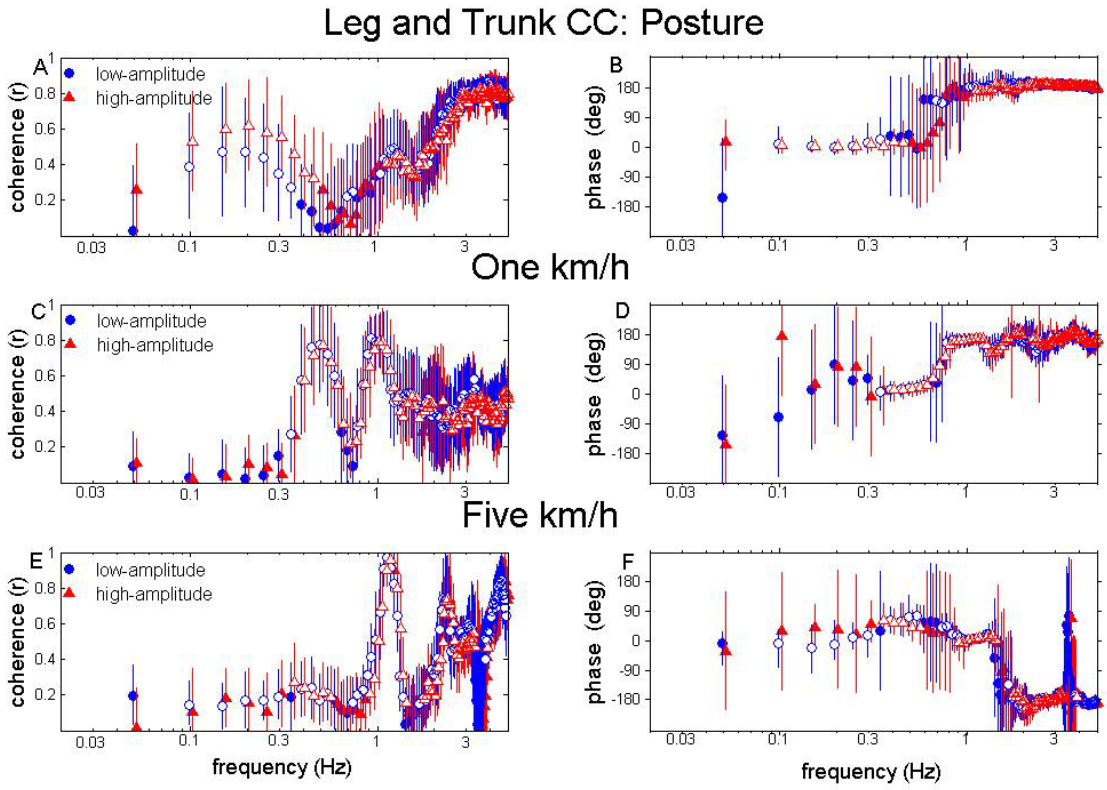

Figure 6.1. Complex coherence of leg and trunk. Complex coherence of leg and trunk. Error bars are 95% confidence intervals (n=12).

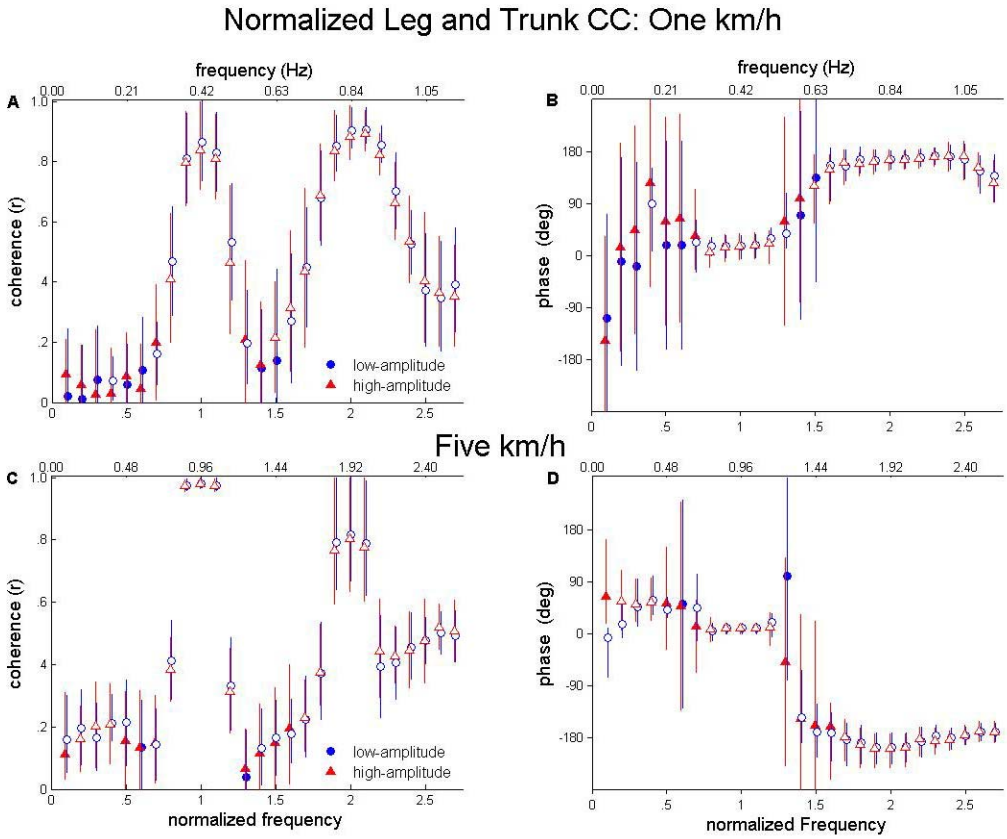

Figure 6.2. Normalized complex coherence of leg and trunk. Complex coherence of leg and trunk normalized to gait frequency. Error bars are 95% confidence intervals (n=12).

Figure 6.2 shows coherence and phase from 0 to 2.7 stride frequency units, which is an appreciable frequency step past the second harmonic of the stride frequency. From this figure, it is clear that these in-phase patterns are centered on the stride frequency and the start of these anti-phase patterns begin near the second harmonic of the stride frequency. In figure 6.2 A-B, the trunk and leg are in-phase from -2 to +2 frequency steps of the stride frequency in the low amplitude condition while being in-phase from -3 to +3 frequency steps of the stride frequency in the high amplitude condition. Anti-phase behavior begins approximately 4 steps prior to the second harmonic of the stride frequency for both low and high amplitude conditions.

Once again, these phases are smaller than 180º as mean phase ±4 steps of the second harmonic is 165 º for the low amplitude and 163º for the high amplitude condition. At 5 km/h, Figure 6.2 C-D shows how the trunk and leg are in-phase from -2 to +2 frequency steps of the stride frequency for both low and high amplitude conditions. Anti-phase behavior begins approximately 5 frequency steps prior to the second harmonic of the stride frequency for the low amplitude condition and 3 steps prior in the high amplitude condition.

Chapter 7: General Discussion

In sum, the behavior of locomotion was probed with visual information to investigate several different processes of postural control that allow upright stability. In chapter 4 it was made clear that there is a separate amplitude space that needs to be probed when attempting to provide evidence of absence or presence of intra-modality reweighting during locomotion. In chapter 5 it was shown that the navigation task of locomotion interferes with the simultaneous maintenance of postural orientation and equilibrium in the trunk. Finally, chapter 6 shows the in-phase and anti-phase behavior of leg-trunk coordination was observed within locomotion, and this coordination is centered at the frequency of gait and its ensuing harmonic.

Intra-modal reweighting not evident in locomotion

After a pilot investigation, it was believed that drastic increases in the response of the body to visual scene motion occur in locomotion compared to standing posture. As a fault of the sum of sines stimulus used, power from the gait cycle and its harmonics interfered with the properties of FRFs at the frequencies of the stimulus. By using a filtered white noise signal in the ensuing experiment, power was spread across frequencies to better understand the effects of the gait cycle on linear frequency domain techniques typically used to study postural control mechanisms. In addressing hypotheses 1-3 that make predictions about reweighting during locomotion, low and high amplitude filtered white noise signals with the same properties were used as visual stimuli in posture and two speeds of locomotion. By using the same amplitudes across posture and speeds of locomotion it was assumed that responses could be measured using the same properties of stimuli at each speed.

Amplitude dependent changes in gain interpreted as intra-modal reweighting were not found in locomotion as expected. In displacements, there were not consistent and real responses to low amplitude conditions at all speeds. When amplitude comparisons were possible, increased gains due to decreasing amplitude were observed more in posture than locomotion conditions. Additionally, more consistent responses in the high amplitude conditions were observed in hip and shoulder kinematics. As these reweighting relationships were tenuous in locomotion, it was not plausible to compare or discuss which portion of the body displayed larger amplitude dependent changes in gain. For segment angles, responses were even more dismal with low amplitude conditions and did not improve in the high amplitude conditions during locomotion. In the end, the most consistent real responses to the visual display were found in the trunk and leg in the posture: high amplitude condition. In all, more consistent responses were seen in displacements in comparison to segment angles and in the trunk in comparison to the lower body.

By normalizing these FRFs to the stride frequency, the effect of the stride frequency on the FRF analysis of a single side was shown. No kinematics had a real response to visual scene motion in the complex plane at the normalized gait frequency. Transfer functions at the ankle had the largest ellipses as the power generated at the feet generates a large amount of power that is non-coherent to the visual display. By plotting these FRFs at the normalized gait frequency it was confirmed that large increases in gain from posture to locomotion can be caused by incoherent power generated by the gait cycle. Indeed, choosing a gait speed for these

types of experiments is choosing where there will be a considerable amount of noise to the response signal that is trying to be detected.

Understanding the influence of the stride frequency motivated the investigation of responses of trunk displacements and segment angle during posture and locomotion that were averaged across both sides of the body. In doing so, power at the gait cycle was reduced as averaging A/P displacements counteracted the effects of transverse rotation. Additionally, cross-covariance functions showed that the trunk angle has qualitatively the same response to visual scene velocity at all phases of the gait cycle, and that the thigh angle is much more dependent on visual information in certain stages of the gait cycle. Although these phase-dependent cross-covariance functions reveal phases of the gait cycle in which velocity information is used by the thigh, they are descriptive here and do not allow much interpretation into the limit-cycle properties of the gait cycle in each condition. These analyses did, however, provide the impetus for using gain and phase of FRFs to separate the postural processes of orientation and equilibrium control in the trunk during locomotion.

Trunk-leg coordination

Previously deemed "co-existing excitable modes" (Creath et al, 2005), the in-phase and anti-phase behavior observed in the complex coherence of leg and trunk during posture has been replicated in Figure 6.1. Interestingly, similar patterns of trunk-leg coordination were observed in locomotion conditions and were altered by speed. Coherences different from zero in one km/h started at a higher frequency range than the start of significant coherences in posture. These significant coherences coupled with phases that approximate 0º show in-phase behavior for both low and

high amplitude conditions. The occurrence of anti-phase behavior at one km/h occurs at a lower frequency than seen in posture and this anti-phase behavior appears oscillatory for the remainder of frequencies observed. At five km/h, consistent in-phase behavior in both amplitudes started at a much higher frequency than posture and one km/h. Additionally, anti-phase behavior began at a much higher frequency than observed in either posture or one km/h. Like one km/h, this anti-phase behavior appears oscillatory for the remainder of frequencies. As the mean stride frequency was .42 Hz for one km/h and .96 Hz for five km/h, these in-phase and anti-phase behaviors were believed to coincide with the stride frequency. Because of this association, normalized complex coherence was computed. After normalizing by the stride frequency, it was shown that these in-phase and anti-phase patterns were centered at the stride frequency and its second harmonic. These leg-trunk coordination patterns are preserved in walking at different speeds, and increasing the stride frequency increases the initial frequency at which these patterns begin.

Such a technique to investigate coordination between the leg and trunk has not been used in locomotion, and the support for such trunk-leg coordination is mostly based in biomechanics. It has been shown that rotation at the shoulder is directly out of phase with the rotations of the pelvis in the transverse plane during walking (Inman et al, 1980). A potential cause of these rotations, balance at the trunk in the plane of progression has been characterized as controlling the counteracting moments caused by weight acceptance and push off to cause inverted pendulum behavior(Winter, MacKinnon, Ruder, & Wieman, 1993). As single inverted pendulum models are often used to describe walking (Farley & Ferris, 1998), it is not a big leap to conclude that

the coordination patterns presented here are a result of a double-link inverted pendulum. Alternatively, there is growing evidence that the segment angles of the leg (I.e. foot, shank and thigh) are elegantly coordinated during walking, and this coordination is due to neural control rather than biomechanical linkages (Borghese, Bianchi, & Lacquaniti, 1996; Ivanenko, d'Avella, Poppele, & Lacquaniti, 2008). Although these authors do not consider the trunk segment's relation to the planar covariation of the leg, it is too early in the investigation of these in-phase and anti-phase coordination patterns to rule out their methodology as implausible or unsupportive.

As approximately two thirds of the body's mass is located above the hip (Winter, 1989), there is the need to understand how the head, arms, and trunk are coordinated with the locomotive apparatus of the legs. The main question here surrounds whether this in-phase and anti-phase behavior represents postural stability within locomotion or a coordinative structure that arises due to the behavior of locomotion. From a postural control view, these in-phase and anti-phase patterns are a moving coexistence of hip and ankle strategy. Alternatively, the swinging arms and legs cause these coordination patterns resulting from the biomechanics of gait.

Conclusion and Future Directions

Admittedly, we have reported this "ego-freeze" illusion coarsely in comparison to the rigorous mathematical descriptions afforded by the pyschophysics literature. Although this scene stabilization was initially a secondary finding in our investigation, we now believe that this perception is tied to motor control processes of the nervous system. Through further manipulations of scene motion (amplitude,

velocity, etc.), we hope to combine the techniques presented here with psychophysical methods to further understand the role of visual perception during locomotion in the context of upright stability.

In addition to investigating the trunk, there are still many unanswered questions regarding the interaction of the gait cycle and postural stability. Consequently, some investigators have used nonlinear techniques to characterize the locomotory stability of the body from gait cycle to gait cycle (Dingwell et al, 2007; Granata & Lockhart, 2008). As responses in the leg to visual scene motion are observed at certain phases of the gait cycle, nonlinear techniques will be required to understand their contribution to upright stability amidst the effects of the gait cycle. To expand upon previous models of the interaction of posture and locomotion (Kay & Warren, 2001), it will be worthwhile to understand the contribution of both the leg and trunk segment to the postural stability component in conjunction with the step to step stability of the gait cycle.

The analyses used in this study point towards an understanding of the harmony of locomotive processes and upright stability. One cannot view postural stability within locomotion without keeping in mind the navigational goals of the nervous system, as the separation of orientation and displacements presented here have shown. Also presented, the coordinative structures that configure the body for locomotion innately contribute to upright stability. In the end, these analyses provide impetus for an increased focus on the use of sensory information in the interaction of translating the body and keeping it upright during the behavior of locomotion.

Appendix 1: Consent Form

FONDAZIONE SANTA LUCIA
ISTITUTO DI RICOVERO E CURA A CARATTERE SCIENTIFICO
Ospedale di rilievo nazionale e di alta specializzazione per la riabilitazione neuromotoria
00179 Roma -Via Ardeatina, 306 - Tel +39 06515011 - Fax +39 065032097 - www.hsantalucia.it

MODULO CONSENSO INFORMATO

Io sottoscritto ..... dichiaro di aver preso visione del protocollo concernente **"Lo studio dell'effetto della stimolazione visiva sul controllo locomotorio nell'uomo"** che si svolgerà presso la Fondazione Santa Lucia.

In particolare dichiaro

- di aver ricevuto, all'interno di tale foglio illustrativo, l'informativa prevista dall'articolo 13 del D.lgs. 196/2003 riguardo al trattamento dei dati personali.
- di avere avuto a disposizione tempo sufficiente per poter leggere attentamente e comprendere quanto contenuto nel suddetto foglio illustrativo.
- di aver ricevuto dai responsabili del progetto che operano presso il Dipartimento di Fisiologia Neuromotoria IRCCS Fondazione Santa Lucia esaurienti spiegazioni in merito alla richiesta di partecipazione allo studio.
- di essere stato informato del diritto di ritirarmi dalla ricerca in qualsiasi momento, senza dover dare spiegazioni.
- Di aver ricevuto il nominativo del Dott. Yura Ivanenko come nominativo del Responsabile dei dati (D.Lgs 196/2003) e della Sperimentazione
- Di aver ricevuto il nominativo del Dott. Gianfranco Bosco o della Dott.ssa Elena Daprati o del Dott. Francesco Lacquaniti come medico referente per qualsiasi ulteriore chiarimento o informazione relativa alla sperimentazione
- Di aver avuto modo di esporre le mie considerazioni e di domandare ulteriori precisazioni, nonché di avere avuto il tempo necessario per prendere una decisione ponderata e non sollecitata.

Pertanto, sono consapevole delle attività previste e delle modalità di una mia adesione.

Ciò premesso dichiaro

di acconsentire ☐
di non acconsentire ☐

a partecipare allo studio ed al conseguente trattamento dei miei dati personali sensibili.

cognome e nome della persona	firma della persona
_____	_____

oppure

cognome e nome del rappresentante legalmente valido	firma del rappresentante legalmente valido
_____	_____
cognome e nome del medico che raccoglie il consenso	firma del medico che raccoglie il consenso
_____	_____

NB: il presente modulo è valido solo se accompagnato dal corrispondente foglio illustrativo

(timbro e firma)

FONDAZIONE SANTA LUCIA
ISTITUTO DI RICOVERO E CURA A CARATTERE SCIENTIFICO
Ospedale di rilievo nazionale e di alta specializzazione per la riabilitazione neuromotoria
00179 Roma -Via Ardeatina, 306 - Tel +39 06515011 - Fax +39 065032097 - www.hsantalucia.it

FOGLIO INFORMATIVO PER LA RICHIESTA DI CONSENSO INFORMATO ALLA PARTECIPAZIONE AD ATTIVITA' DI RICERCA SCIENTIFICA ED AL CONSEGUENTE TRATTAMENTO DEI DATI PERSONALI

Gentile Signore/a .....

la Fondazione Santa Lucia è un Istituto di Ricovero e Cura riconosciuto a Carattere Scientifico, che svolge, insieme all'attività di assistenza, quella di ricerca sanitaria e di formazione nel settore della riabilitazione neuromotoria e delle neuroscienze.

Nell'ambito di tale esercizio, è programmato lo svolgimento di una ricerca dal titolo **"Lo studio dell'effetto della stimolazione visiva sul controllo locomotorio nell'uomo"**.

Lo studio prende in considerazione l'effetto della stimolazione visiva sul controllo del cammino nell'uomo e si prefigge di analizzare le modificazioni che intervengono nella normale deambulazione, quando durante il cammino viene presentata una particolare stimolazione visiva attraverso lo studio della cinematica e dell'attività elettromiografica di superficie durante il cammino sul tapis roulant.

I benefici previsti non saranno specificamente diretti per il partecipante ma potranno concretizzarsi in un aumento delle conoscenze specifiche di questo settore.

Non sono previsti rischi per le persone che partecipano allo studio e Lei in ogni momento può interrompere l'esperimento o fare una pausa, dicendo allo sperimentatore, che è sempre presente accanto a Lei, la sua intenzione.

Con il presente modulo Le viene proposto di prendere parte al programma di studio, il cui responsabile scientifico è il Dott. Yury Ivanenko.

Se Lei deciderà di partecipare allo studio, sarà inserito, dopo la raccolta dei suoi dati da parte del personale addetto, nel gruppo sperimentale.

L'impegno a Lei richiesto per partecipare allo studio consiste nell'eseguire diversi compiti motori come camminare su di un tapis roulant a diverse velocità (1-3-5-7 km/h), camminare sul posto e postura mentre a 1-2 m da lei, su di uno schermo, è proiettata una scena visiva. L'immagine sullo schermo è costituita da piccoli triangoli bianchi su fondo nero che si muovono avanti e indietro. Verranno registrate anche alcune prove mentre Lei è sottoposto ad una leggera forza di trazione sul tronco attraverso un torque-motor. Un filo rigido e leggero sarà attaccato tramite una cintura posteriormente al tronco mentre l'altra estremità sarà attaccata al torque-motor comandato da un computer. L'estremità del filo rigido attaccata a Lei è provvista di un dispositivo di sicurezza che controlla la forza esercitata dal torque-motor ed in caso di raggiungimento del limite massimo stabilito tale dispositivo interviene svincolandoLa. Durante tutto lo svolgimento dell'esperimento Lei indosserà un leggero giubbotto collegato attraverso una corda di sicurezza al soffitto che andrà in tensione in modo tale da evitare eventuali cadute accidentali. Il tapis roulant è dotato di diversi dispositivi di sicurezza. Delle barre fisse laterali forniscono un appoggio che Lei può utilizzare in ogni momento durante l'esperimento, un grande pulsante rosso posizionato davanti a Lei ferma lo scorrimento del tappeto se vuole fermarsi e smettere di camminare ed inoltre è presente un meccanismo (calamita di sicurezza staccabile facilmente in caso di rischio) tramite il quale se Lei va troppo indietro rispetto alla lunghezza del tapis roulant il movimento del tappeto rallenta e si ferma. La durata del Suo impegno è prevista in circa 2h 30min.

Il medico referente, nella persona del Dott. Gianfranco Bosco o della Dott.ssa Elena Daprati o del Dott. Francesco Lacquaniti, sarà sempre a Sua disposizione per qualsiasi chiarimento. La

informerà prontamente di qualunque notizia si renda disponibile durante lo studio e provvederà a sospendere la Sua partecipazione allo studio qualora ciò risulti nel suo interesse, comunicandoLe i motivi di tale sospensione.

Nel corso dello studio al quale prenderà parte, Lei sarà assicurato a copertura di eventuali danni da esso derivante.

La partecipazione allo studio non comporta per Lei alcun aggravio di spesa.

Lo studio è stato approvato dal Comitato Etico Indipendente della Fondazione Santa Lucia ed il suo svolgimento ed i suoi risultati sono monitorati dallo stesso Comitato.

Nel caso di accettazione a partecipare allo studio, Lei ha il diritto di ritirarsi dallo stesso in qualsiasi momento, senza essere obbligato a fornire alcuna giustificazione.

Si precisa che i risultati dello studio verranno portati a conoscenza della comunità scientifica ed i dati raccolti durante la sperimentazione non potranno rimanere di proprietà di singoli o gruppi che li possano utilizzare secondo il loro esclusivo interesse.

La procedura dello studio garantisce, peraltro, la riservatezza dei Suoi dati personali con riferimento al relativo Codice (D.lgs. del 30 giugno 2003, n. 196), ai sensi del cui art. 13 si sottopone la seguente informativa.

in conformità alle disposizioni del Codice in materia di protezione dei dati personali (di seguito "Codice"), la Fondazione Santa Lucia La informa che intende svolgere attività di trattamento di dati personali (di seguito "Dati"), anche sensibili[1]*, che La riguardano.*

FINALITA' E MODALITA' DEL TRATTAMENTO DEI DATI

I Dati forniti vengono acquisiti e trattati nel rispetto della normativa sopra richiamata, con il supporto di mezzi cartacei, informatici o telematici atti a memorizzare, gestire e trasmettere i dati stessi e comunque mediante strumenti idonei a garantire la loro sicurezza e riservatezza, nel rispetto delle regole fissate dal Codice, per le finalità della ricerca in precedenza descritta riguardo agli obiettivi, alle procedure, ai benefici ed rischi della partecipazione, all'impegno operativo e temporale richiesto

NATURA DEL CONFERIMENTO E CONSEGUENZE DI UN EVENTUALE RIFIUTO

L'eventuale rifiuto di fornire i Dati funzionali all'esecuzione della ricerca su menzionata, non comporta alcuna conseguenza relativamente ad eventuali trattamenti terapeutici in corso, salva l'eventuale impossibilità di dare seguito alle operazioni connesse alla ricerca.

Lei è libero/a di non partecipare alla ricerca o di ritirarsi dallo stessa anche senza preavviso o motivazione. Qualora, durante la ricerca, divengano disponibili dati che possano influenzare la Sua volontà di continuare Lei sarà tempestivamente ed opportunamente informato e, se necessario, Le sarà richiesto nuovamente il Consenso Informato a proseguire il trattamento in corso.

COMUNICAZIONE DEI DATI

I Dati potranno inoltre venire a conoscenza dei responsabili della cui opera la Fondazione Santa Lucia si avvale nell'ambito di rapporti di

[1] L'art. 4 del Codice definisce "*sensibili*" i dati personali idonei a rivelare l'origine razziale ed etnica, le convinzioni religiose, filosofiche o di altro genere, le opinioni politiche, l'adesione a partiti, sindacati, associazioni od organizzazioni a carattere religioso, filosofico, politico o sindacale, nonché i dati personali idonei a rivelare lo stato di salute o la vita sessuale.

esternalizzazione per la fornitura di servizi, nonché dei responsabili e degli incaricati del trattamento dei dati per le finalità di cui alla presente informativa, l'elenco aggiornato dei quali è a disposizione presso la sede della Fondazione Santa Lucia.

I Dati relativi ai risultati della ricerca sono strettamente confidenziali e soggetti ad anonimato. I risultati potranno essere portati a conoscenza di terzi o pubblicati, ma escludendo ogni possibile riferimento personale al paziente

DURATA DEL TRATTAMENTO

I Dati verranno trattati dalla Fondazione Santa Lucia solamente per la durata della ricerca. La durata complessiva della ricerca è prevista di 5 anni.

DIRITTI DELL'INTERESSATO

L'art. 7 del Codice riconosce all'interessato numerosi diritti che La invitiamo a considerare attentamente. Tra questi, Le ricordiamo sinteticamente i diritti di:

- *ottenere la conferma dell'esistenza o meno dei Dati che lo riguardano, anche se non ancora registrati, e la loro comunicazione in forma intelligibile;*
- *ottenere l'indicazione dell'origine dei Dati, delle finalità e modalità del trattamento, degli estremi identificativi del titolare, dei responsabili, dei soggetti o delle categorie di soggetti ai quali i Dati possono essere comunicati o che possono venirne a conoscenza in qualità di responsabili o incaricati;*
- *ottenere l'aggiornamento, la rettificazione o l'integrazione dei Dati (qualora vi sia un interesse in tal senso) ovvero la cancellazione, la trasformazione in forma anonima o il blocco dei dati trattati in violazione di legge, nonché l'attestazione che tali operazioni sono state portate a conoscenza di coloro ai quali i Dati sono stati comunicati o diffusi;*
- *opporsi, in tutto o in parte, al trattamento dei Dati che lo riguardano per motivi legittimi ovvero per fini di invio di materiale pubblicitario o di vendita diretta o per il compimento di ricerche di mercato o di comunicazione commerciale.*

Lei, per l'intera durata del trattamento, potrà chiedere informazioni o porre domande al medico circa i dati acquisiti nel corso della sperimentazione e circa l'andamento della stessa relativamente al suo caso; allo stesso modo, al termine della ricerca, se richiesto, i risultati che La riguardano saranno comunicati a Lei ed al suo medico di base.

TITOLARE DEL TRATTAMENTO

Titolare del trattamento è la Fondazione Santa Lucia, Via Ardeatina 306 Roma

Per qualsiasi ulteriore informazione, chiarimento e comunicazioni a disposizione Il responsabile dei dati è: Yura Ivanenko

Dott. Responsabile della sperimentazione: Yura Ivanenko

Reparto: Dipartimento di Fisiologia Neuromotoria, Laboratorio della Locomozione

Firma

Roma, li ……

……

Bibliography

Antonsson, E. K. & Mann, R. W. (1985). The frequency content of gait. *J.Biomech., 18,* 39-47.

Bauby, C. E. & Kuo, A. D. (2000). Active control of lateral balance in human walking. *J.Biomech., 33,* 1433-1440.

Borghese, N. A., Bianchi, L., & Lacquaniti, F. (1996). Kinematic determinants of human locomotion. *J.Physiol, 494 (Pt 3),* 863-879.

Bruggeman, H., Zosh, W., & Warren, W. H. (2007). Optic flow drives human visuo-locomotor adaptation. *Curr.Biol., 17,* 2035-2040.

Cenciarini, M. & Peterka, R. J. (2006). Stimulus-dependent changes in the vestibular contribution to human postural control. *J.Neurophysiol., 95,* 2733-2750.

Creath, R., Kiemel, T., Horak, F., Peterka, R., & Jeka, J. (2005). A unified view of quiet and perturbed stance: simultaneous co-existing excitable modes. *Neurosci.Lett., 377,* 75-80.

Cromwell, R. L., Pidcoe, P. E., Griffin, L. A., Sotillo, T., Ganninger, D., & Feagin, M. (2004). Adaptations in horizontal head stabilization in response to altered vision and gaze during natural walking. *J.Vestib.Res., 14,* 367-373.

Deshpande, N. & Patla, A. E. (2005). Dynamic visual-vestibular integration during goal directed human locomotion. *Exp.Brain Res., 166,* 237-247.

Deshpande, N. & Patla, A. E. (2007). Visual-vestibular interaction during goal directed locomotion: effects of aging and blurring vision. *Exp.Brain Res., 176,* 43-53.

Dickinson, M. H., Farley, C. T., Full, R. J., Koehl, M. A., Kram, R., & Lehman, S. (2000). How animals move: an integrative view. *Science, 288,* 100-106.

Dingwell, J. B. & Cusumano, J. P. (2000). Nonlinear time series analysis of normal and pathological human walking. *Chaos., 10,* 848-863.

Dingwell, J. B. & Marin, L. C. (2006). Kinematic variability and local dynamic stability of upper body motions when walking at different speeds. *J.Biomech., 39,* 444-452.

Donelan, J. M., Shipman, D. W., Kram, R., & Kuo, A. D. (2004). Mechanical and metabolic requirements for active lateral stabilization in human walking. *J.Biomech., 37,* 827-835.

Durgin, F. H., Gigone, K., & Scott, R. (2005). Perception of visual speed while moving. *J.Exp.Psychol.Hum.Percept.Perform., 31,* 339-353.

England, S. A. & Granata, K. P. (2007). The influence of gait speed on local dynamic stability of walking. *Gait Posture, 25,* 172-178.

Farley, C. T. & Ferris, D. P. (1998). Biomechanics of walking and running: center of mass movements to muscle action. *Exerc.Sport Sci.Rev., 26,* 253-285.

GIBSON, J. J. (1958). Visually controlled locomotion and visual orientation in animals. *Br.J.Psychol., 49,* 182-194.

Granata, K. P. & England, S. A. (2006). Stability of dynamic trunk movement. *Spine, 31,* E271-E276.

Hashiba, M. (1998). Transient change in standing posture after linear treadmill locomotion. *Jpn.J.Physiol, 48,* 499-504.

Hicheur, H., Vieilledent, S., & Berthoz, A. (2005). Head motion in humans alternating between straight and curved walking path: combination of stabilizing and anticipatory orienting mechanisms. *Neurosci.Lett., 383,* 87-92.

Hollands, M. A., Patla, A. E., & Vickers, J. N. (2002). "Look where you're going!": gaze behaviour associated with maintaining and changing the direction of locomotion. *Exp.Brain Res., 143,* 221-230.

Hollands, M. A., Ziavra, N. V., & Bronstein, A. M. (2004). A new paradigm to investigate the roles of head and eye movements in the coordination of whole-body movements. *Exp.Brain Res., 154,* 261-266.

Horak, F. B. & Macpherson, J. M. (1996). Postural orientation and equilibrium. In J.Shepard & L. Rowell (Eds.), *Handbook of Physiology* (pp. 255-292). New York: Oxford University Press.

Inman, V., Alston, H., & Todd, F. (1981). *Human Walking*. Baltimore: Williams and Wilkins.

Ivanenko, Y. P., d'Avella, A., Poppele, R. E., & Lacquaniti, F. (2008). On the origin of planar covariation of elevation angles during human locomotion. *J.Neurophysiol., 99,* 1890-1898.

Kang, H. G. & Dingwell, J. B. (2006). A direct comparison of local dynamic stability during unperturbed standing and walking. *Exp.Brain Res., 172,* 35-48.

Kay, B. A. & Warren, W. H., Jr. (2001). Coupling of posture and gait: mode locking and parametric excitation. *Biol.Cybern., 85,* 89-106.

Kiemel, T., Elahi, A. J., & Jeka, J. J. (2008). Identification of the plant for upright stance in humans: multiple movement patterns from a single neural strategy. *J.Neurophysiol., 100,* 3394-3406.

Kiemel, T., Oie, K. S., & Jeka, J. J. (2006). Slow dynamics of postural sway are in the feedback loop. *J.Neurophysiol., 95,* 1410-1418.

Konczak, J. (1994). Effects of optic flow on the kinematics of human gait: a comparison of young and older adults. *J.Mot.Behav., 26,* 225-236.

Kuo, A. D. (2007). The six determinants of gait and the inverted pendulum analogy: A dynamic walking perspective. *Hum.Mov Sci., 26,* 617-656.

Lamontagne, A., Fung, J., McFadyen, B. J., & Faubert, J. (2007). Modulation of walking speed by changing optic flow in persons with stroke. *J.Neuroeng.Rehabil., 4,* 22.

MacKinnon, C. D. & Winter, D. A. (1993). Control of whole body balance in the frontal plane during human walking. *J.Biomech., 26,* 633-644.

Mahboobin, A., Loughlin, P. J., Redfern, M. S., & Sparto, P. J. (2005). Sensory re-weighting in human postural control during moving-scene perturbations. *Exp.Brain Res., 167,* 260-267.

Mesland, B. S. & Wertheim, A. H. (1996). A puzzling percept of stimulus stabilization. *Vision Res., 36,* 3325-3328.

Mulavara, A. P. & Bloomberg, J. J. (2002). Identifying head-trunk and lower limb contributions to gaze stabilization during locomotion. *J.Vestib.Res., 12,* 255-269.

Nashner, L. M. (1982). Analysis of Stance Posture in Humans. In A.L.Towe & E. S. Luschei (Eds.), *Handbook of Behavioral Neurobiology* (New York: Plenum Press.

Oie, K. S., Kiemel, T., & Jeka, J. J. (2002). Multisensory fusion: simultaneous re-weighting of vision and touch for the control of human posture. *Brain Res.Cogn Brain Res., 14,* 164-176.

Pavard, B. & Berthoz, A. (1977). Linear acceleration modifies the perceived velocity of a moving visual scene. *Perception, 6,* 529-540.

Peterka, R. J. (2002a). Sensorimotor integration in human postural control. *J.Neurophysiol., 88,* 1097-1118.

Peterka, R. J. & Benolken, M. S. (1995). Role of somatosensory and vestibular cues in attenuating visually induced human postural sway. *Exp.Brain Res., 105,* 101-110.

Probst, T., Brandt, T., & Degner, D. (1986). Object-motion detection affected by concurrent self-motion perception: psychophysics of a new phenomenon. *Behav.Brain Res., 22,* 1-11.

Prokop, T., Schubert, M., & Berger, W. (1997). Visual influence on human locomotion. Modulation to changes in optic flow. *Exp.Brain Res., 114,* 63-70.

Rossignol, S., Dubuc, R., & Gossard, J. P. (2006). Dynamic sensorimotor interactions in locomotion. *Physiol Rev., 86,* 89-154.

Sarre, G., Berard, J., Fung, J., & Lamontagne, A. (2008). Steering behaviour can be modulated by different optic flows during walking. *Neurosci.Lett., 436,* 96-101.

Schubert, M., Bohner, C., Berger, W., Sprundel, M., & Duysens, J. E. (2003). The role of vision in maintaining heading direction: effects of changing gaze and optic flow on human gait. *Exp.Brain Res., 150,* 163-173.

Thurrell, A. E. I., Pelah, A., & Distler, H. K. (1998). The influence of non-visual signals of walking on the perceived speed of optic flow. Perception 27, 147-148. Ref Type: Abstract

Thurrell, A. E. I. & Pelah, A. (2002). Reduction of perceived visual speed during walking: effect dependent upon stimulus similarity to the visual consequences to locomotion. Journal of Vision 2, 628a. 7-20-0009. Ref Type: Abstract

Vallis, L. A. & Patla, A. E. (2004). Expected and unexpected head yaw movements result in different modifications of gait and whole body coordination strategies. *Exp.Brain Res., 157,* 94-110.

Varraine, E., Bonnard, M., & Pailhous, J. (2002). Interaction between different sensory cues in the control of human gait. *Exp.Brain Res., 142,* 374-384.

Warren, W. H., Kay, B. A., & Yilmaz, E. H. (1996). Visual control of posture during walking: functional specificity. *J.Exp.Psychol.Hum.Percept.Perform., 22,* 818-838.

Wertheim, A. H. & Reymond, G. (2007). Neural noise distorts perceived motion: the special case of the freezing illusion and the Pavard and Berthoz effect. *Exp.Brain Res., 180,* 569-576.

Winter, D. A. (1989b). Biomechanics of normal and pathological gait: implications for understanding human locomotor control. *J.Mot.Behav., 21,* 337-355.

Winter, D. A. (1989a). Biomechanics of normal and pathological gait: implications for understanding human locomotor control. *Journal of motor behavior, 21,* 337.

Winter, D. A., MacKinnon, C. D., Ruder, G. K., & Wieman, C. (1993). An integrated EMG/biomechanical model of upper body balance and posture during human gait. *Prog.Brain Res., 97,* 359-367.

Zhang, Y., Kiemel, T., & Jeka, J. (2007). The influence of sensory information on two-component coordination during quiet stance. *Gait Posture, 26,* 263-271.

Zijlstra, W., Rutgers, A. W., & Van Weerden, T. W. (1998). Voluntary and involuntary adaptation of gait in Parkinson's disease. *Gait Posture, 7,* 53-63.

Zoubir, A. & Boashash, B. (1998). The bootstrap and its application in signal processing. *IEEE Signal Processing Magazine, 15,* 56-76.